Rocket stability assessment

CFD analysis of fin shapes and their impact on the static
stability of a sounding rocket

Bachelor thesis

Bachelor of Science in Aviation

Author	Alexander Schoch
Supervised by	Dr. Pierluigi Capone
	Andrea Pedrioli
In cooperation with	ARIS
Date	June 9. 2023

DECLARATION OF ORIGINALITY

Project report at the School of Engineering

By submitting this report, the undersigned student confirms that this thesis is his/her own work and was written without the help of a third party. (Group works: the performance of the other group members are not considered as third party).

The student deClares that all sources in the text (inCluding Internet pages) and appendices have been correctly disClosed. This means that there has been no plagiarism, i.e. no sections of the Bachelor thesis have been partially or wholly taken from other texts and represented as the student's own work or inCluded without being correctly referenced.

Any misconduct will be dealt with according to paragraphs 39 and 40 of the General Academic Regulations for Bachelor's and Master's Degree courses at the Zurich University of Applied Sciences (Rahmenprüfungsordnung ZHAW (RPO)) and subject to the provisions for disciplinary action stipulated in the University regulations.

City, Date: **Name Student:**

Zurich, 09.06.2023   _____

                                            Alexander Schoch

Abstract

This bachelor thesis was conducted in collaboration with the student research group ARIS. The purpose of this paper is to analyze the aerodynamic characteristics of the Helvetia sounding rocket with three different fin shapes. Two of the fin designs are provided by ARIS whereas the last design is an original creation that was aimed to be an optimized draft compared to the previous designs. The fins are evaluated in terms of lift, drag and effect on the center of pressure in supersonic condition. The goal is to find which fin design is most suitable for the Helvetia rocket. This study is performed by conducting CFD simulations. Ultimately, it was discovered that the original Helvetia fin proves to be the most suitable. However, given the lessons learned, implementing certain refinements to the internal design has the potential to surpass the efficiency of the Helvetia fin. This would need to be confirmed in future studies. Lastly, the second ARIS fin proved to be unsuitable for the Helvetia rocket.

Keywords: CFD, sounding rocket, static stability

Table of Contents

List of Abbreviations

A.o.a – Angle of attack

ARIS – Akademische Raumfahrt Initiative Schweiz

BOI – Body of influence

CFD – Computational fluid dynamics

Cl = coefficient of lift

Cd = coefficient of drag

CP – Center of pressure

CG – Center of gravity

ISA – International Standard Atmosphere

Max q – maximum dynamic pressure

Re – Reynolds number

ZHAW – Zürcher Hochschule für Angewandte Wissenschaften

List of figures

1 Introduction

Aerospace technologies are often associated with being original, efficient and cutting edge. However, this often comes along with high costs and selective working positions. Despite all that, the student non-profit organization ARIS, Akademische Raumfahrtinitiative Schweiz [1], offers young engineering students the possibility to put theory into practice by working on space related engineering projects. In that regard, students may work on the development of a sounding rocket for international competition, contribute to long term projects such as cubesats or contribute their own research in the form of a thesis.

This paper is one such thesis which is written as part of the ZHAW Bachelor of Science in Aviation. Specifically, this thesis focuses on the performance and optimization of rocket fins. The aim is to post process previous ARIS rocket launches in order to draw an independent conclusion on the rocket's performance and to contribute the knowledge gained to future projects. The intended approach is to analyze the rocket's static stability and how it is affected by fin shape and size.

The evaluation of the stability of any airborne vehicle is crucial for a successful operation. However, in order to reliably assess the stability parameters of an aircraft an extensive study must be conducted. In general, there are three different methods that are applied to perform such studies. Firstly, analytical methods can be used. The Barrowman equation [2], which will be mentioned later in this paper is an example for analytically determining the CP of a rocket. Secondly, there are computational methods. Computational fluid dynamics or CFD is the approach to numerically solve the complex equations of fluid dynamics. Lastly, the stability of an aircraft can be assessed experimentally. This is the most reliable one of the aforementioned methods. Commonly, this Includes wind tunnel testing. However, conducting experimental test flights is also a possibility [3].

Nonetheless, while an experimental evaluation may yield the most reliable results, it conversely is also the most expensive one [4]. For small startup companies or student associations it is virtually impossible to access such infrastructure. Especially when the aircraft is developed to operate at supersonic speeds. Therefore, it is of great interest for such companies to find efficient alternatives. As a result, some very significant equations that can be solved analytically started appearing during the last century. As mentioned, the Barrowman equations [2], are one example. However, also simplified forms of the Navier-Stokes equation can be used to analytically solve problems in fluid dynamics. For example, the fluid flow around a sphere for slow flow speeds can be analytically expressed by solving the Stokes equations in steady state condition [5]. However, for more complex geometries the analytical methods reach their limits quite quickly. Consequently, numerical methods for solving more complex problems in fluid dynamics become significantly more attractive. On the other hand, CFD simulations require a substantial amount of computational power. Thus, similarly to wind tunnel testing, historically CFD analysis used to be out of reach for the general public. However, given the remarkable progress in computer technology it is now possible to run CFD simulations on one's own laptop.

However, despite the increasing availability of CFD software and suitable hardware, CFD simulations can still be hard to tackle. It takes a substantial amount of time and patience to understand the intricacies of the available CFD tools.

Most likely due to the compact time schedule the competition teams at ARIS are limited to, only a few CFD studies were internally conducted. Therefore, the engineers at ARIS relied on analytical methods. A powerful tool which is frequently used by ARIS members is Open Rocket [6]. Open Rocket is an open-source software which allows the user to make trajectory simulations for their rocket, find the CP, the static margin and more. However, according to the Open Rocket wiki [6], the software produces unreliable results at supersonic flow speeds. Moreover, this raises the question of reliability regarding the static margin which is a critical indicator on the static stability of any rocket [2]. In addition, according to the rocket competition regulations [7], the rocket must fulfill a certain static margin requirement in order to be allowed to launch.

Therefore, within the scope of this thesis a thorough CFD analysis of the Helvetia sounding rocket is performed. The goal of this thesis is to compare the Open Rocket results with the ones gathered with CFD. The focus lies on the determination of static stability during peak velocity of the rocket flight. In addition, drag and lift coefficients are also determined. Hence, an overview of the rocket's aerodynamic performance will be gained. In a proceeding step, the performance of the Helvetia fins will be compared to a previous model called Piccard. Piccard was ARIS's second supersonic rocket which suffered an uncontrolled tumble after reaching its apogee [8]. The motivation behind analyzing a previous design is to gain some insight into fin optimization. Lastly, the lessons learned from Helvetia and Piccard are used to find an optimized fin shape. Using the preliminary fin design, the CFD analysis is repeated. Ultimately, all fins are compared and a conclusion in regard to the fin's performance will be drawn.

2 Literature Review

The following section contains a summary of the theory that was applied to this thesis.

2.1 CFD

Y+

Y+ is a dimensionless number that can help determine the size of the initial inflation layer of a mesh in order to properly solve the turbulent flow around a wall. According to Salim M. et al [9], for flow with high Reynolds number, as is the case in this paper, one needs to rely on logarithmic wall functions. Those functions rely on the so called "law of the wall", [10] which is an equation derived from empirical data. It states that for most turbulent flows the velocity distribution near a wall is very similar. For such wall functions a Y+ value between 30 – 300 is desired. This is significant as it can help to drastically reduce the total amount of cells in a mesh and hence the computational power required to solve it. If no wall function were used the Y+ value would need to be close to 1. This results in an exponentially larger mesh.

Given this information, Schlichtig and Gersten [10], denote the relation between Y+ and the initial distance to the wall as follows:

$$y^+ = \frac{y u_\tau}{\nu}$$

(1)

For this project a Y+ value of 200 was aimed at. Thus, given the equation above one can solve for y to find the initial inflation layer height. In order to find the initial cell size after the inflation layer one must define a grow rate as well as the number of layers. The initial cell size can then be found with the following equation [10].

$$y' = y \cdot r^n$$

(2)

Where *y'* is the first cell size, *r* the grow rate and *n* the amount of inflation layers.

Pressure far field

In short, a pressure far field is a boundary condition within the CFD software that simulates an infinite space, in contrast to modelling a wind tunnel. [11] For that reason, the geometry for the mesh that captures this field must be large enough so that no wall interference other than with the tool body itself is experienced. Moreover, the PFF cannot be used for fluids with constant density. In other words, this boundary condition is most suitable for supersonic simulations where compressibility is a significant factor. [12]

Some key aspects of the PFF that need to be considered are the following.

Initially, the fluid flow speed is defined by setting a certain Mach number. Furthermore, to replicate an a.o.a, the Mach number magnitude can be decomposed into a vertical as well as a horizontal component. See equations 3, 4 [12] for determining the correct values for a certain a.o.a.

$$vertical\ component = \sin{(a.o.a)}$$

(3)

$$horizontal\ component = \cos{(a.o.a)}$$

(4)

In addition, the PFF requires a gauge pressure input as well as a thermal component. Essentially, those parameters are the static - pressure and temperature that are required to calculate the density, as well as the fluid flow speed. In case only the total temperature or pressure respectively are known, one must rely on the perfect gas law to determine the correct values. The following equations needed to be applied for the first CFD case.

Firstly, the relation between stagnation and static pressure can be expressed in terms of Mach number as follows, [13]:

$$\frac{T_0}{T} = 1 + \frac{\gamma - 1}{2}M^2$$

(5)

Given this equation one can solve for T to find the static temperature. For finding the static pressure one can rely on the relation between temperature and pressure derived from the equation of state, [13].

$$\frac{p_0}{p} = \frac{T_0^{\frac{\gamma}{(\gamma-1)}}}{T}$$

(6)

Given the equation of state:

$$p = \rho RT$$

(7)

One can find the fluid density as well.

Cl and Cd evaluation

Given the intricacies of the PFF, it is important to understand how to evaluate the results gathered during the simulations. Primarily, within the scope of this thesis, this includes the proper estimation of the Cd and Cl values. In theory, the Cl and Cd values found by the CFD software are more accurate in contrast to applying an analytical method. Moreover, according to Seeni and Rajendran, [14] the lower the Reynolds number, the more accurate the desired results are. However, for the results to be

precise, the mesh for the simulation must be Close to perfect. Moreover, even though their case employed a low Re-number model their results showed some discrepancies, nonetheless. Therefore, especially since the Re-number in this project is far greater than in Seeni's and Rahendran's case, [14] it was decided to use an analytical method to estimate the lift and drag coefficients.

The equation employed for analytically finding the Cd and Cl values were the common lift and drag equations seen bellow, [15]:

$$L = 0.5 * cl * \rho * V_\infty^2 * S$$

(8)

$$D = 0.5 * cd * \rho * V_\infty^2 * A$$

(9)

The CFD solver was set up to find the forces acting in Z as well as in X direction. See figure 1 for the chosen coordinate system. Hence, when an a.o.a is introduced, a conversion equation must be employed to determine the lift and drag components from the forces acting along the X- and Y-axes, respectively, as depicted in figure 1. The equations used for this conversion can be seen bellow.

$$FL = Fz \cdot \cos(a.o.a) - Fx \cdot \sin(a.o.a)$$

(10)

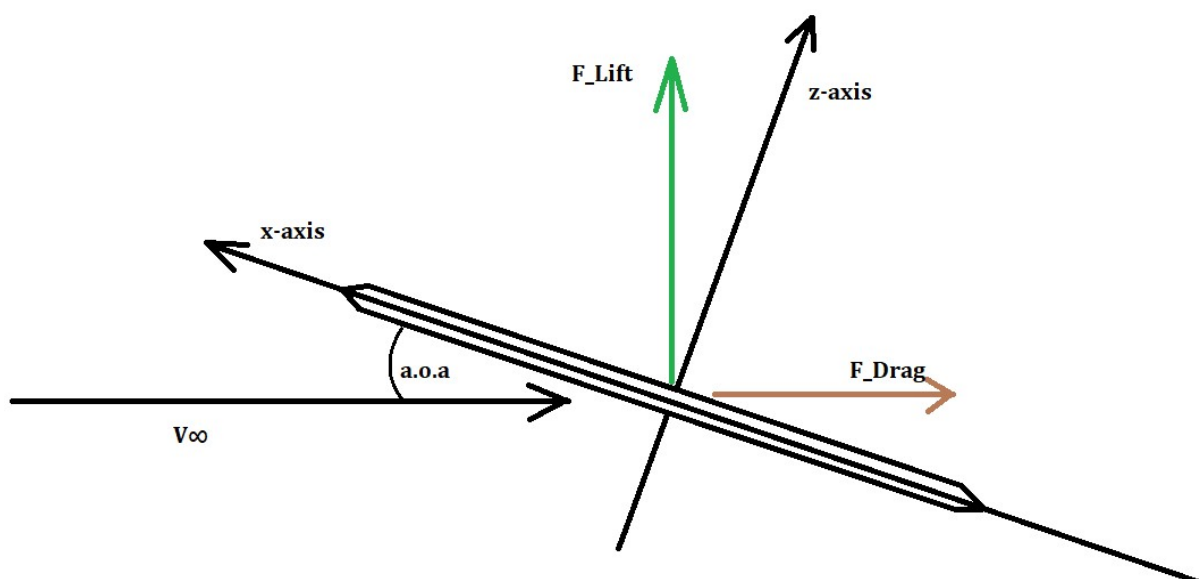$$FD = Fx \cdot \cos(a.o.a) + Fz \cdot \sin(a.o.a)$$

(11)

Figure 1 Coordinate system and forces within PFF.

Prandtl-Glauert transformation

In order to gain some insight into the aerodynamic characteristics of the fins at subsonic flight conditions the so called Prandtl-Glauert transformation can be applied. As stated in Andersen's Fundamentals in Aerodynamics [16], the physics between subsonic and supersonic flight are entirely different. Hence, no direct conversion of Cl and Cd values from supersonic to subsonic condition can be made. However, there are equations to approximate such a transition. By deriving the linearized perturbation velocity potential (equation 12) one finds equation 13, where equation 14 is the Prandtl-Glauert factor. The derivation of equation 12 is beyond the scope of this thesis. Nonetheless, as stated in Andersen's book one can find that CP, Cl and cm coefficients are affected by a factor of one over the Prandtl-Glauert factor β when transitioning from supersonic to subsonic condition. Ultimately, equation 14 will be applied later in this thesis.

linearized perturbation velocity potential:

$$(1 - M_\infty^2)\frac{\partial^2 \hat{\phi}}{\partial x^2} + \frac{\partial^2 \hat{\phi}}{\partial y^2} = 0$$

(12)

Prandtl-Glauert factor:

$$\beta = \sqrt{1 - M_\infty^2}$$

(13)

Cl approximation equation:

$$Cl = \frac{Cl_0}{\beta}$$

(14)

It is important to note that this approximation is valid only for small angles of attack, a slim plate airfoil, similarly to a fin and lastly, the perturbation in Mach number must be within the transonic range. For larger changes in Mach number there is no guarantee for accurate results [17].

Nonetheless, this approximation will be used to demonstrate the Cl decrease when transitioning into the supersonic regime. Lastly, the approximation will be done to give an approximate lift curve for subsonic speeds.

2.2 Sweep angle of fins

The idea behind creating a fin that has a sweep angle is to delay the formation of shock waves on the surface of the fin. Therefore, drastically reducing the amount of drag that is produced. Moreover, as soon as the critical Mach number is surpassed the drag starts to increase exponentially until the free stream velocity passes Mach 1 [18]. The critical Mach number is the free stream velocity at which the flow over the surface over a fin breaks the sound barrier. The critical Mach number is usually around 5% to 10% below the free stream Mach number.
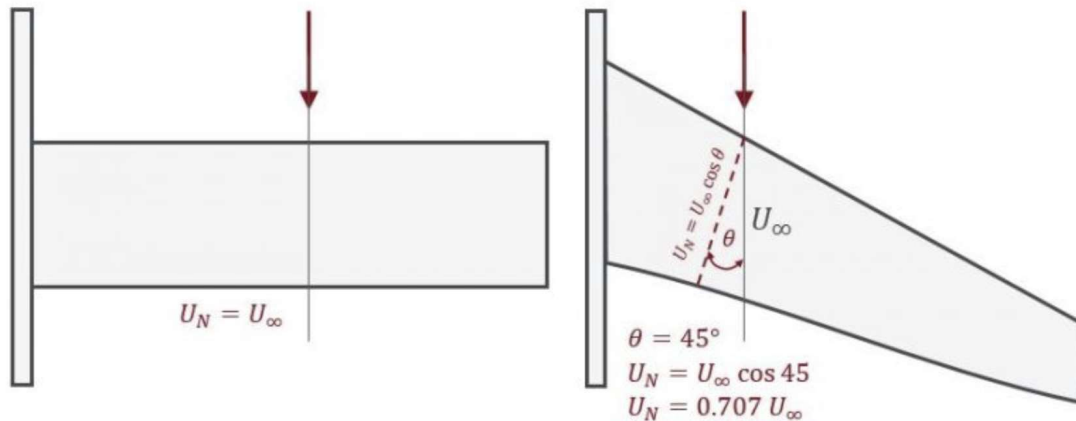

Figure 2 Relation between sweep angle and critical Mach number [18]

Figure 2 demonstrates the relation between the sweep angle and the reduced flow velocity over the wing U_N. In this case, a 45° sweep can reduce the flow velocity over the wing by almost 30%. Moreover, assuming an M_{crit} of 0.9 one can solve the equation in figure 2 for U_∞. As a result, one finds that for a sweep angle of 45°, M_{crit} is not reached before a free stream velocity of Mach 1.27. Importantly, one must note that the reduced flow velocity also creates less lift [18].

2.3 Static stability

Static stability of an aircraft refers to the tendency of the aircraft to return to its original state or position once it's been disturbed. A statically stable object will always return to its origin, an unstable object will accelerate away from its origin and lasty, a neutrally stable object will continue on its path with constant velocity. Importantly, the static stability refers to a single timeframe [19]. Regarding rocket technology the term static stability is Closely related to the static margin. The static margin is calculated by dividing the distance between the CP and CG by the rocket's tube diameter [20]. A positive static margin indicates a stable rocket whereas a negative one suggests that the rocket is unstable. In other words, the CP must be behind the CG in order to have a statically stable rocket. It is the job of the rocket fins to shift the CP behind the CG of the rocket. Moreover, the static margin must be chosen according to the desired operating capabilities. For instance, a marginally stable rocket can be highly manoeuvrable and less susceptible towards wind gusts. However, it also means that it can quickly become unstable as the center of pressure tends to move forwards with an increase in angle of attack [20]. Thus, reducing the static margin. However, a large

static margin means that the rocket will tend to become overstable. This effect can be compared to a weathervane which will always point towards the incoming wind. Similarly, as soon as gust strike the rocket it will deviate from its flight path, potentially compromising the mission. According to the ARIS Helvetia technical report, [7] the static margin should lie within 2-6. Otherwise, the rocket is not Cleared for take-off. Lastly, a large angle of attack causes the CP to move rearwards once again. The reason for this the flow starts to transition from laminar to turbulent. The flow separation occurs first at the trailing edge and then moves forwards with an increase in a.o.a. This turbulent air creates a larger pressure drop than when the flow is laminar. The angle of attack at which this rewards shift in center of pressure becomes noticeable is called the critical angle of attack. [16] Although the CP shifts rearwards and theoretically increases the static margin, it is important to note that this does not mean that the rocket is more stable. In contrary, the delamination of the airflow results in less lift as well as an increase in drag. The determination of the critical angle of attack is important in the design of an aircraft and is part of the fin investigation within this thesis.

Lastly, the center of pressure is essentially the average location of pressure along the rocket [2]. Hence, it is also the point at which the aerodynamic forces act. Therefore, the moment at this point must be zero. This is a valuable characteristic that will be exploited in determining the CP position at various angles of attack.

OpenRocket

The OpenRocket simulator is a powerful open-source software. It was originally developed by Sampo Niskanen as part of their Master thesis [21]. Since then, it has been constantly updated. It allows the user to implement a simplified CAD model of virtually any rocket geometry. Its capabilities lie within immediately calculating the rocket's center of pressure as well as center of gravity. Hence determining the rocket's static margin. Moreover, it's possible to implement rocket motors and simulate the rocket's trajectory. Regarding the CP the software relies on a combination of analytical methods as well as empirical data. In terms of analytical methods, namely the Barrowman equations are implemented. The equations found by James S. Barrowman [2], allow to find a variety of aerodynamic coefficients based on the rocket's geometry. However, according to Barrowman, [2] the equations are limited to an accuracy of 10% for speeds between Mach 2 and 8. For subsonic speeds Barrowman states that a similar discrepancy can be expected. Moreover, as mentioned, OpenRocket takes empirical models into account. These models include correction factors for surface roughness, fin shape and component interference. Thus, increasing the accuracy of the simulation. Nonetheless, OpenRocket was designed primarily for model rockets. [20], [21].

In conclusion, although the software is a powerful, user-friendly tool, it's primarily dedicated to model rockets. For a more detailed analysis a more advanced aerodynamic analysis tool, such as CFD, is usually employed. Ultimately, this thesis aims to analyse and find the extend of the discrepancies between OpenRocket and CFD.

3   Research Goal

Primary objective

The main goal of this thesis is to create several robust CFD models of the Helvetia sounding rocket in supersonic condition. Specifically, three different fin shapes are to be implemented in the CFD models. The aim is to find the aerodynamic characteristics of those fins when attached to the Helvetia rocket. In addition, the first two fins are previous ARIS designs whereas the last fin is an own design that aims to be an optimized version of the preceding fins.

The desired results include firstly, finding the lift and drag curves for each fin over an angle of attack ranging from 0° to 30°.

Secondly, the static margin when exposed to the mentioned range of angles of attack is to be determined for each configuration.

Ultimately, it should be possible to make a verdict on the advantages and shortcomings of each fin.

Secondary objective

In addition, there are two secondary goals.

Firstly, the results from the CFD simulations are to be compared with the OpenRocket software. The aim is to disclose whether OpenRocket is sufficiently accurate to be used by ARIS.

Secondly, a preliminary study is to be conducted by replicating a NASA wind tunnel test of a missile with a CFD simulation. The intention is to validate the accuracy of the own CFD simulations. For this, the lift and drag of the fins as well as the overall static stability is to be again examined.

4 Data Collection & Research Methods

In pursuit of the stated objective, the tools employed included OpenRocket [20] and the CFD software ANSYS fluent [12]. The approach remained largely consistent for the various fin shapes that were investigated. Firstly, a CAD model of the rocket including the fins was designed. Secondly, the CFD simulation was set up and finally executed. During the post processing of the simulation the lift and drag forces for various angles of attack were extracted. In addition, the center of pressure is determined for every a.o.a by finding the position of zero pitching moment. Simultaneously, the rockets with the various fin shapes are modelled in OpenRocket. By extracting the CP and cg position from OpenRocket the static margin can be found. Ultimately, the following points are investigated for each different fin shape:

- The Coefficient of lift and coefficient of drag with respect to angles of attack ranging from 0° to 30°.
- The change of center of pressure location depending on angle of attack.
- The Static stability of the rocket in relation to various angles of attack.
- A Comparison between the static margin results of OpenRocket and the CFD simulations.

The results are listed in chapter 5. The following chapters contain a more detailed account for each rocket case.

4.1 NASA validation case

ARIS engineers use OpenRocket in order to find their rocket's static margin as well as to simulate the rocket's flight trajectory. However, a lift and drag analysis in relation to a change in a.o.a is not done. Therefore, there is no empirical data to compare the CFD results of this project with. Consequently, it was decided to choose a validation case to ensure that correct lift, drag and CP locations can be found with CFD. In addition, the validation case should provide an insight into the margin of error that must be expected with CFD analysis.

For the validation case, a wind tunnel investigation of a supersonic missile conducted by NASA was chosen. In this 1978 study, [22], the missile's aerodynamics were investigated with free stream Mach numbers from 1.7 to 2.86 and an angle of attack ranging from 0° to 25°.
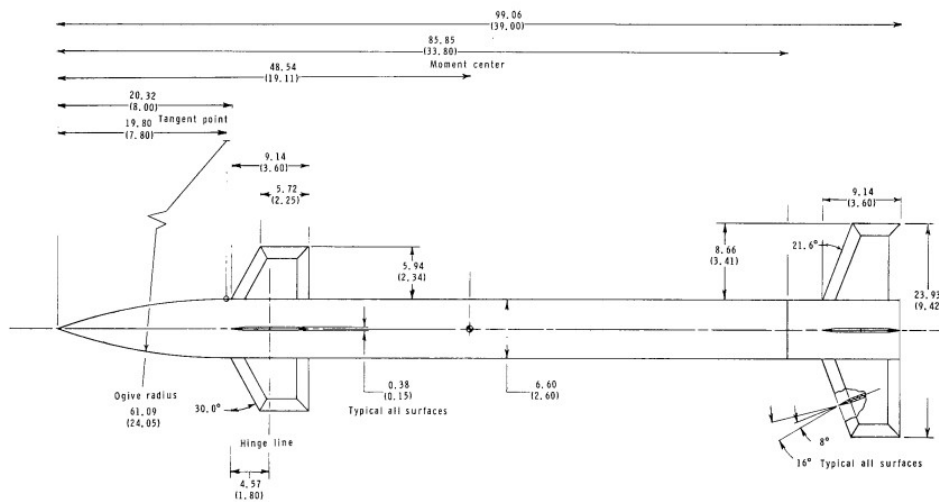
Figure 1.- Model details. All dimensions are in centimeters (inches) unless otherwise indicated.

Figure 3 Dimensions of NASA missile [22]

The dimensions of the missile were provided within the paper. See figure 3. Thus, as a first step a CAD model of the missile was created. This was done with ANSYS SpaceClaim [23]. In a next step the CAD was prepared for the upcoming meshing process. As the free stream velocity reaches supersonic speeds, it was decided to apply a pressure far field boundary condition. Thus, according to the ANSYS FLUENT user guide [12], a fluid sphere with a diameter of twenty times the object length was created around the missile. Subsequently, two bodies of influence, BOI, were created around the missile. The inner BOI has a width only slightly wider than the missile, however, twice as long in order to capture the expected turbulence. The second BOI is three times larger than the inner BOI. The reason for creating such bodies is to allow manual control over the cell size in that region during the meshing process. Lastly, the entire geometry was cut in half. This was done in order to save computational power, as the object is symmetrical. Hence, the same results can be expected on either side of the symmetry plane. This concludes the set up prior to meshing.

For the mesh the internal ANSYS meshing software was used. The approach to meshing was to start with the cell dimensions of the inner BOI. As mentioned in the literature section of this paper the cell size was chosen according to the values found by solving the boundary layer given a Y+ value of 200. In this case, by applying equations 1 and 2 the initial inflation layer was $4.5*10^{-4}$m wide. A grow rate of 1.2 was chosen together with 14 inflation layers. Therefore, a cell width of 0.006m was chosen for the inner BOI. The outer BOI's cells were chosen to be three times the size of the inner BOI with a width of 0.018m. Moreover, the sizing for the pressure far field was left on default. Ultimately, all faces of the rocket were sized as well. The rocket was split into subparts consisting of the fins, the nosecone, the boattail and the rest of the rocket. Those subparts were then sized independently. The sizing was chosen according to the solver's ability to create the inflation layer. Initially all faces were sized with a width slightly larger than the initial inflation layer height. However, whenever the

14

solver created a stairstep mesh in some areas, as can be seen in figure 7, the face needed to be sized even finer.

Eventually, this resulted in a cell count of 3 502 124 cells. The final mesh can be seen in figure 27 in the appendix. This concludes the mesh set up.

Lastly, the mesh was exported into the ANSYS fluent solver. The NASA paper [22] provided information about total pressure, total temperature as well as Mach number. As mentioned before, according to the ANSYS fluent user guide [12], a PFF boundary condition requires static pressure as well as static temperature as an input. Those values were determined by applying equations 5 and 6. The static pressure was calculated to be 11426 Pa and the static temperature 215 K. Importantly, the operating conditions need to be set to 0 Pa pressure without gravity. The reason for this is that the fluid domain is created according to the reference values, if the PFF is chosen as the reference domain. In addition, the flow direction can be defined by applying horizontal, as well as vertical components. Therefore, an a.o.a can be created by applying equations 3 and 4. Moreover, according to the PFF requirements, the fluid material must be set to an ideal gas [12]. Furthermore, the energy equation was turned on and lastly, the SST k-omega solver was chosen as the simulation's viscous model. This concludes the setup of the solving process.

Ultimately, several simulations were executed while the a.o.a was changed each time. The output for each simulation was a lift and drag force for the fins, as well as a pitching moment along the entire rocket. The reason for finding the pitching moment is to determine the rocket's center of pressure. As mentioned in chapter 2.3 the rocket's pitching moment should be zero at the rocket's CP. Thus, in order to find the correct location, the pitching moments were calculated for several positions along the body axis of the rocket. Lastly, the coefficients of lift as well as the coefficient of drag needed to be determined. This was done analytically, as it proved to be more reliable than directly using the ANSYS solver. In order to find those coefficients equations 8 and 9 were applied. Importantly, the reference area of the missile fins needs to be divided by two given that only half of the rocket's geometry was used for simulation.

For all following CFD cases the set-up procedure of the solver software is nearly identical.

Mesh sensitivity study

In order to be sure that a mesh can produce reasonable results it is common practice to perform a mesh sensitivity study. This is mostly done by setting up an initial mesh and then iteratively increasing the cell count. Hence, making the mesh finer. The results in question should then converge to a certain value. This process is repeated until the difference between the results are within a certain margin. The mesh that fulfills this margin will then be chosen for the simulations. There are several guidelines that suggest that the mesh has reached a reasonable accuracy once the difference between two meshes is no more than 1% [24].

Within the scope of this thesis this mesh study was performed for the NASA validation case only. The reason being that such a study is substantially time consuming. Moreover, there are other indicators that can give insight into the quality of the mesh.

Those include the convergence during initialization, the convergence of the residuals and the quality of the mesh in terms of orthogonality, aspect ratio and more [24]. Thus, it was decided to use the NASA validation case as a benchmark. The mesh parameters for the following cases were chosen according to this benchmark. However, the quality of the mesh was judged according to the other mentioned indicators.

OpenRocket

The modelling of rockets within the software is intuitive and will not be further discussed in this thesis. The geometry was modelled according to the geometry from the NASA paper [22] which can be seen in figure 3. The CP location was then evaluated automatically for an angle of attack of 0°. The CG position was approximated by implementing a mass point. By iteratively changing the magnitude of the mass point the correct CG position can be implemented.

Post processing

During post processing there are three key points that need to be evaluated. Firstly, the Cl and Cd values needed to be determined for the various angles of attack. The coefficients were found by applying the mentioned method in chapter 2.1. For simplicity a Matlab script was written that incorporated equations 10 and 11. From the simulations the forces in X and Z direction were extracted and put into the script. Ultimately, the Prandtl-Glauert transformation was also applied on the found values, see equation 14, as mentioned in chapter 2.1. Therefore, enabling a comparison of lift curves under both supersonic and subsonic conditions. The conversion occurred between Mach 1.2 and Mach 0.9. Hence the Prandtl-Glauert factor equals 0.436.

Secondly, the center of pressure needed to be determined. As mentioned in chapter 2.3 the center of pressure can be found at the point of the rocket where the moment is zero. For simplification, even though the CFD simulations are three dimensional, the evaluation of the moment can be regarded as two dimensional. This is because no lateral forces are applied. Hence, the moment in question is the pitching moment and the point of the CP must be along the longitudinal axis of the rocket. In ANSYS one can calculate the moment around an axis at any point along the rocket geometry. Therefore, an initial calculation was conducted at the point at which OpenRocket suggested the CP to be. From there the calculation location was iteratively shifted until the resulting moment equaled zero Newtons. This process was repeated for any change in a.o.a.

Lastly, the Y+ values were evaluated. This can be done with an integrated function in ANSYS. This allows the user to see which Y+ values were reached along the wall of the geometry.

4.2 Helvetia

For this simulation as well as the proceeding ones, the static pressure was chosen according to the trajectory simulations the engineers at ARIS conducted. Altitude, velocity as well as acceleration predictions can be seen in figure 4.
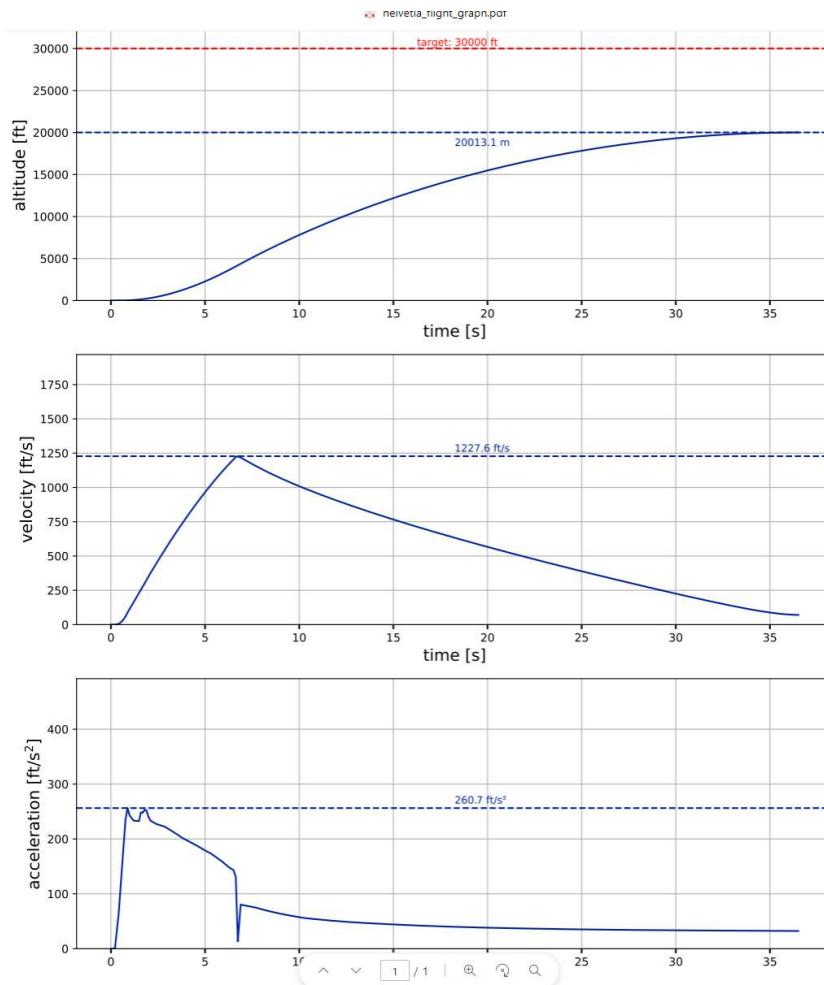
Figure 4 Helvetia trajectory simulations from ARIS [7]

As the peak velocity also indicates the point of maximum dynamic pressure the corresponding altitude can be read from the chart. However, during Helvetia's flight the rocket exceeded the target altitude of 30'000 ft slightly. Therefore, regarding static pressure, a compromising 68770 Pa were chosen which are equivalent to 10'000 ft in ISA conditions.

As mentioned, the CFD process for the various fin shapes was nearly identical as for the NASA canard missile. Therefore, it will not be further discussed in this section. However, for the OpenRocket modelling of the rocket the correct static margin needed to be implemented. This was done by referring to the static margin estimated by ARIS as can be seen in figure 5.

ARIS implemented two different models to approximate the static margin. For the static margin at 0° a.o.a the more conservative value of 3.3 body callipers was chosen rather than the estimate 4 body callipers. Ultimately, by implementing a mass point in the OpenRocket model the static margin was set to 3.3. This can be seen in figure 14 later in the results section.
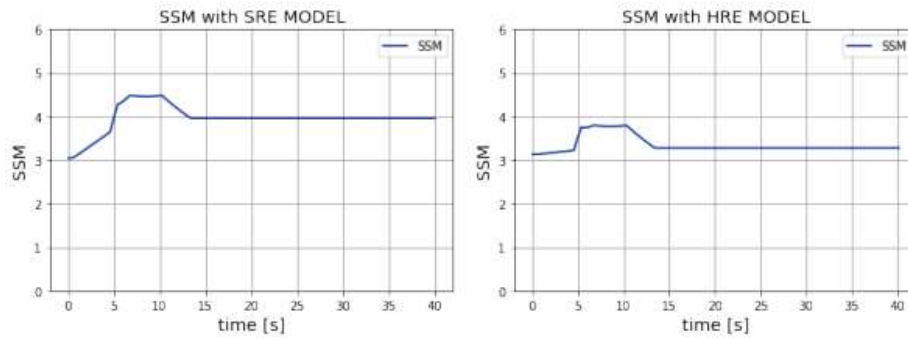
Figure 5 static margin estimation conducted by ARIS [7]

4.3 Piccard

The Piccard fin was designed according to the technical drawings provided by ARIS [8]. Moreover, the CFD setup is nearly identical to the previous setups. Lastly, a static margin of 2 body callipers was estimated by ARIS for the Piccard fin configuration. Therefore, as done in the previous simulation this static margin was implemented into OpenRocket by adjusting a mass point.

4.4 Swept back – Parallelogram

The swept back fin design in the shape of a parallelogram was an in-house design. To find an optimized fin shape the theory discussed in chapter 2.2 was applied. The approach was to find the optimal sweep angle at which the drag is minimized during max q. However, the fin should also provide sufficient lift. The Helvetia sounding rocket surpasses the transonic regime for a short time to reach its peak velocity of Mach 1.2. Therefore, it was decided to sweep the fin just as much so that the critical Mach number is not reached before the rocket reaches Mach 1.2. Furthermore, as no M_{crit} was available it was conservatively chosen to be 0.9. Lastly, as can be seen in equation 16, the sweep angle was found to be 41.4°

$$\theta = cos^{-1}\left(\frac{U_N}{U_\infty}\right)$$

<div align="right">(15)</div>

Where $U_N = M_{crit}$ therefore:

$$\theta = cos^{-1}\left(\frac{0.9}{1.2}\right) = 41.4°$$

<div align="right">(16)</div>

For the swept back fin configurations, a static margin of 3.3 was chosen once again as it was done for the Helvetia fins.

5   Results

In the subsequent section, the outcomes from the CFD simulations are presented. Firstly, the NASA validation case is shown, followed by the examination of the individual cases featuring diverse fin shapes. Ultimately, the different fins are presented in comparison with each other.
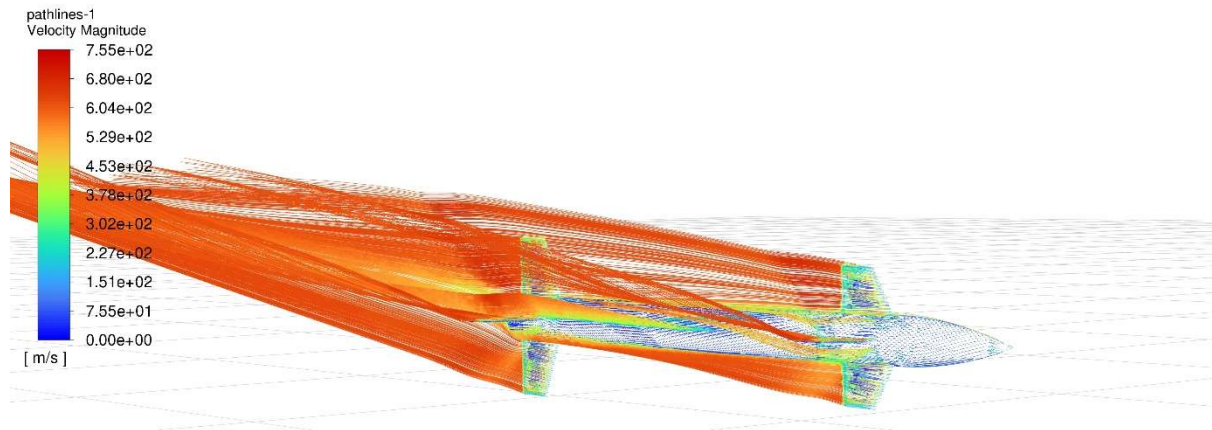
5.1   Nasa canard validation

Figure 6 Pathline illustration of the velocity magnitude of the NASA canard missile at Mach 1.7 and 5° a.o.a
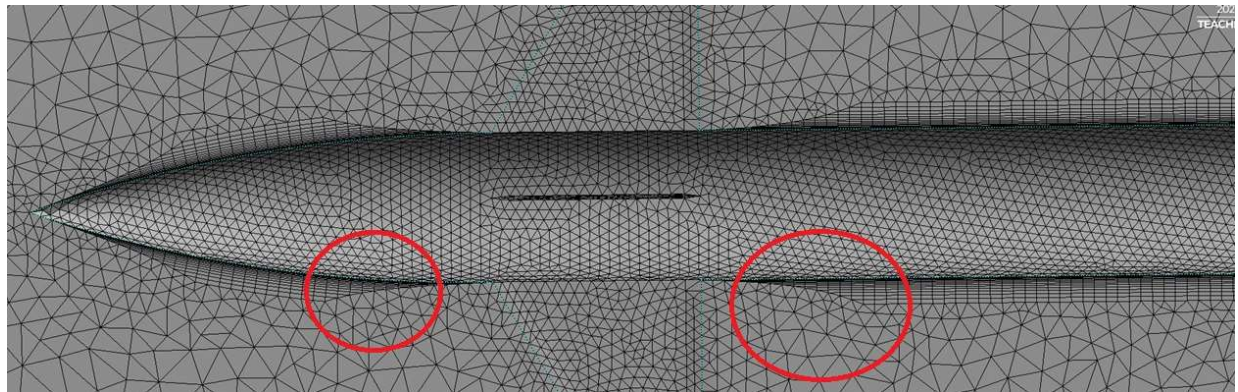
Mesh sensitivity study

Figure 7 NASA Canard missile mesh with Airstep mesh at various locations

The initial mesh had 850 692 individual cells. However, although the solution converged, there were several issues with the mesh that had an impact on the integrity of the results. As can be seen in table 1, the results from the coarsest mesh are about 5% higher than the proceeding finer mesh. The next finer mesh already had four times the cells as the coarsest mesh. While the solution converged as well, there were issues with the inflation layer as can be seen in figure 7. The software created so called Airstep mesh which are indicated with the red circles. Consequently, the boundary layer was not completely resolved for the whole missile. The only way to resolve this

was by making the cells smaller in those areas. Therefore, a last mesh was created with 3 500 000 cells. This mesh yielded results that deviated only 1-2% from the previous mesh and therefore, it was accepted for the entirety of the simulations.

Mesh size	850 692	2 756 374	3 502 124
Fz at 5° a.o.a	91.89 N	86.31 N	85.495 N
Fx at 5° a.o.a	32.27 N	26.72 N	25.58 N
CP at 5°	0.412 m	0.453 m	0.478 m

Table 1 Results from mesh sensitivity study

In addition to the mesh sensitivity study one can see the orthogonal quality of the mesh in figure 8. It is visible that the mean of the cells is within a value of 0.75 for orthogonal quality. Lastly, figure 25, which can be found in the appendix shows the convergence and the residuals of the finest mesh.
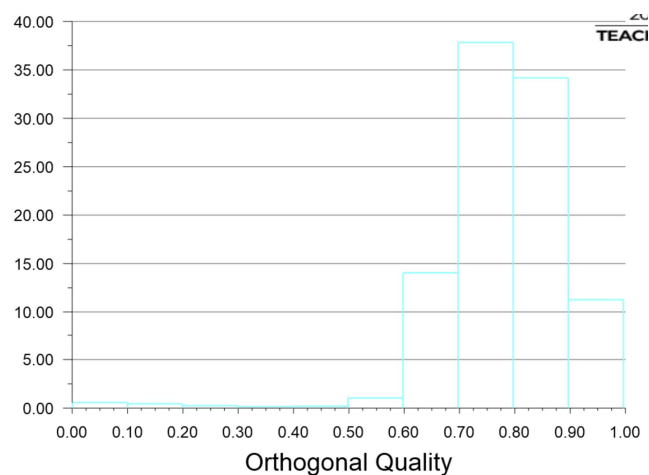
Figure 8 Orthogonal mesh quality of finest Nasa Canard mesh

Lastly, the Y+ values along the wall of the missile were between 1.33 and 2.6 with some stray values reaching 13. See figure 28 in the appendix.
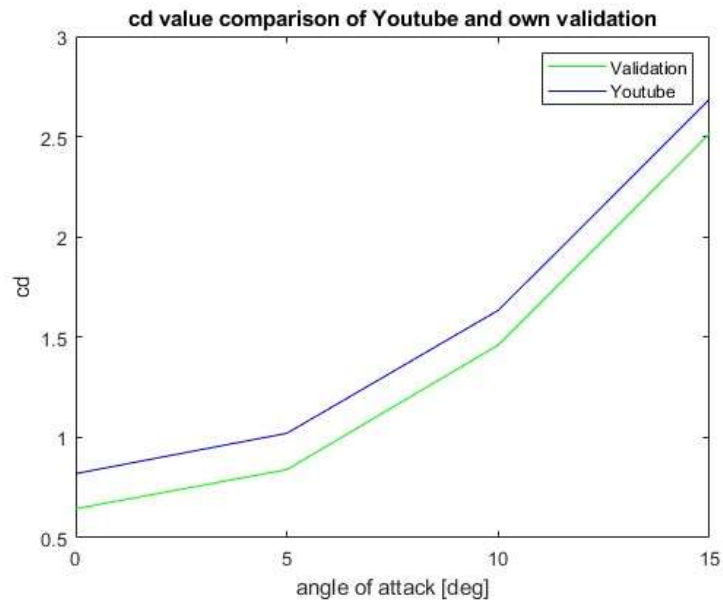
Aerodynamics

Figure 9 Cd values of Youtube CFD reference case and own CFD simulation

Figure 9 shows the coefficient of drag in relation to angle of attack. One can see that the gradients of the own simulation and the online case values are very similar. However, the magnitude of the values yields a difference of 10-15%. As no Cd curve was published during the NASA wind tunnel test only the own CFD analysis and the Youtube case are compared.
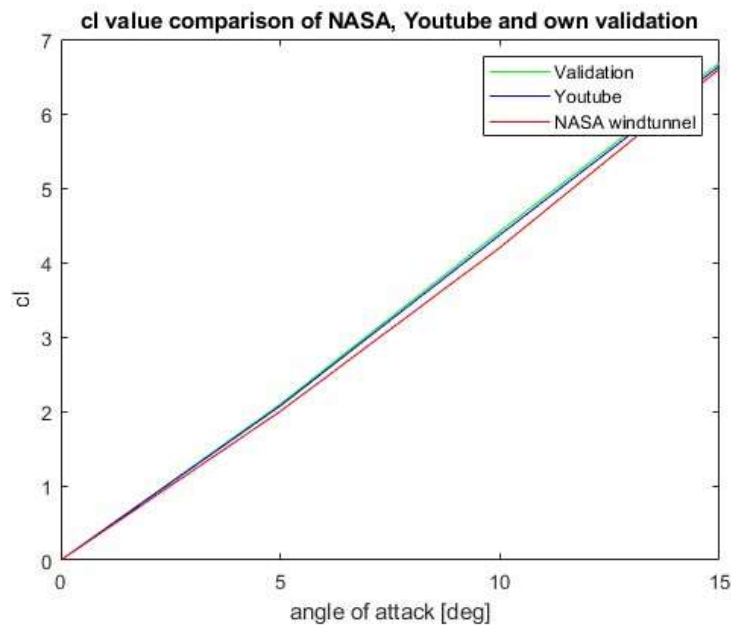

Figure 10 coefficient of lift comparison between the wind tunnel test, Youtbe CFD case and own CFD simulation

21

Figure 10 displays the Cl values over a.o.a. The Cl values for the NASA wind tunnel case are generally slightly lower than those of the CFD cases. Furthermore, the CFD cases exhibit almost identical results. The maximum discrepancy occurs at 10° a.o.a with a difference of 5%. Lastly, even at 15° angle of attack there is no drop in lift.
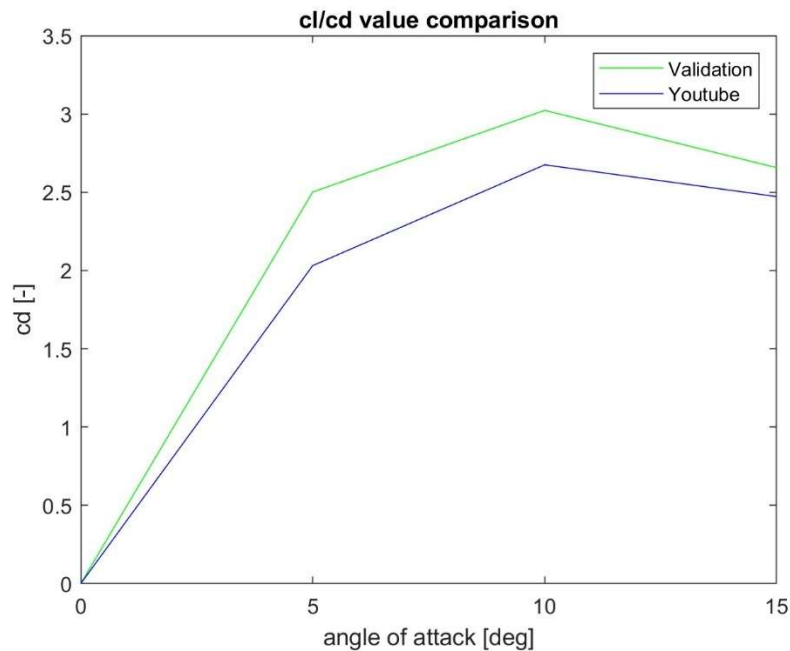

Figure 11 Cl over Cd comparison between reference Youtube CFD case and own CFD simulation

Figure 11 shows the Cl over Cd curves for the Youtube case and the own CFD evaluation. Once again, the gradients are very similar. However, the actual values differ. The maximum drag of the own CFD simulation exceeds the reference drag coefficient by almost 20%.
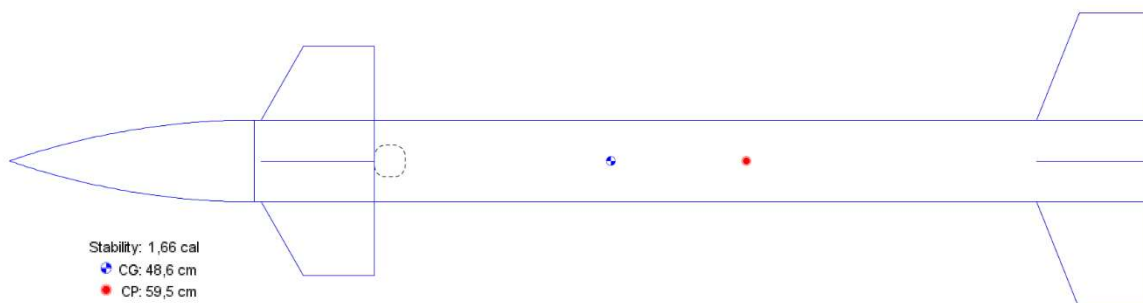

Figure 12 OpenRocket model of canard missile. CP in red and CG in blue

Lastly, the static stability. As can be seen in figure 12, OpenRocket estimated the location of the CP to be at 59.5cm from the tip of the missile. The CG position was taken from the NASA paper [22]. This results in a static margin of 1.66 callipers.
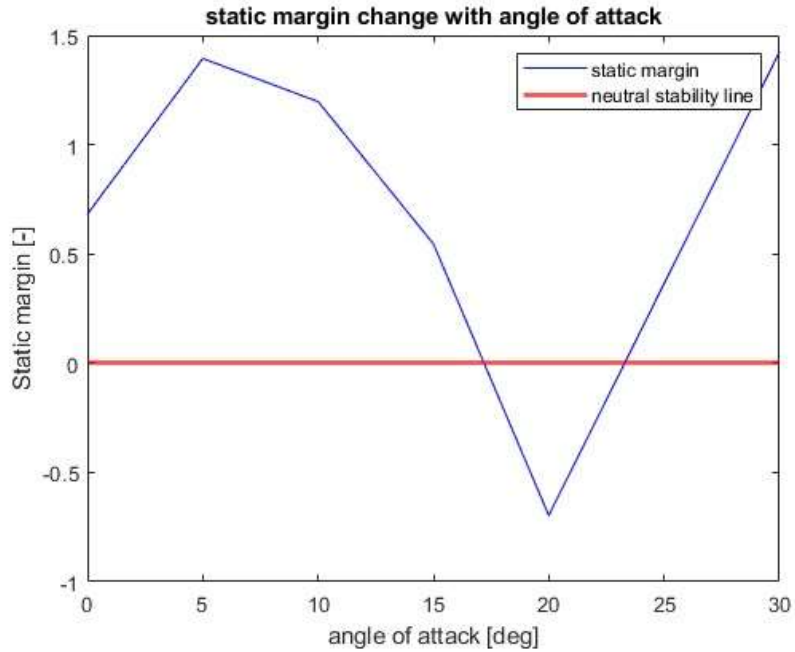
Figure 13 Graph of the change in static margin in relation with a change in a.o.a for the NASA canard missile

The location of the CP according to the CFD simulations with change in a.o.a can be seen in figure 26 in the appendix. The resulting static margin in relation to the change in angle of attack can be seen in figure 13. One can see that initially the CP moves backwards, hence increasing the static margin. However, at 5° a.o.a the CP starts shifting forwards until the point of neutral stability is passed at 17° a.o.a. After 20° a.o.a the CP moves rearwards again.

5.2 Helvetia fins

CFD

Even though the geometry of the Helvetia rocket is almost ten times larger than the Canard missile, it required less cells to achieve converging results. In total the Helvetia mesh, which can be seen in figure 33 in the appendix, has 2 680 566 cells. Moreover, the mean orthogonal quality has a value of 0.78. In addition, the Y+ values lie between 8 to 20. Lastly, the residuals which give insight into the convergence of the results show low values. The highest residual shows a value of 10^-3. The residuals can be seen in the appendix in figure 34.

Aerodynamics

Stability: 3,28 cal
- CG: 304 cm
- CP: 363 cm

Figure 14 OpenRocket model of the Helvetia sounding rocket with Helvetia fin configuration

Open rocket estimated the CP location at 3.63 meters from the tip of the rocket. However, as can be seen in figure 29 in the appendix the CP location from the CFD simulation is initially 0.5 meters further behind. Furthermore, as the a.o.a increases the CP shifts forwards but never reaches the CP location estimated by OpenRocket. After 15° a.o.a the CP moves rearwards again.
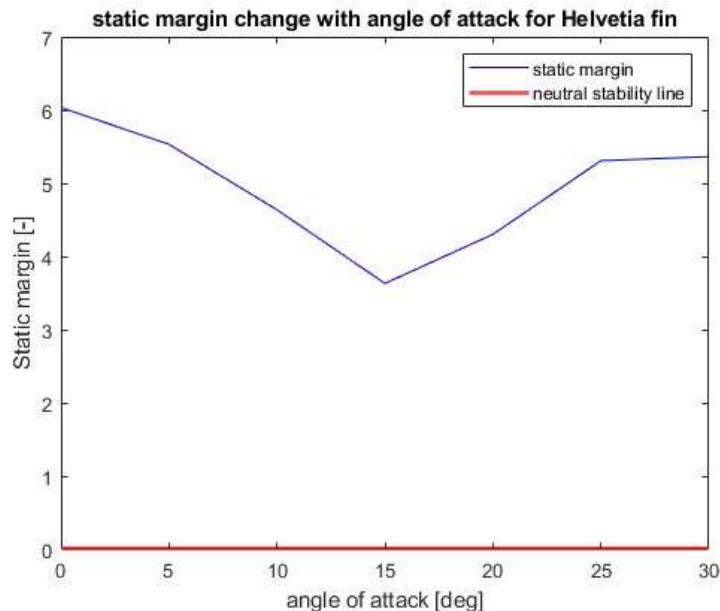

Figure 15 Static margin change in correlation to change in angle of attack for Helvetia fin

Figure 15 shows the resulting static margin over a.o.a. The values never drop below 3.3 and the maximum lies at 6.

5.3 Piccard fins

CFD

The Piccard CFD required 3 626 434 cells. This resulted in a mean Orthogonality of 0.8. The calculations converged after 100 iterations. However, although all residuals show values bellow 10^-3, the energy residual showed a not converged status. The Y+ values lied within 7 and 21.

Aerodynamics

Stability: 2 cal
CG: 344 cm
CP: 380 cm

Figure 16 OpenRocket model of the Helvetia sounding rocket with Piccard fin configuration

The Piccard fins were from the start the ones that provided the lowest static margin. However, as can be seen in figure 17 the CP lied initially behind the OpenRocket estimate. On the other hand, at an angle of attack of 15° the CP shifted to 3.7 meters. As can be seen in 30 in the appendix, this resulted in the lowest static margin with a value of 1.4. As with the Helvetia fins the CP moves rearwards after an angle of attack of 15°.
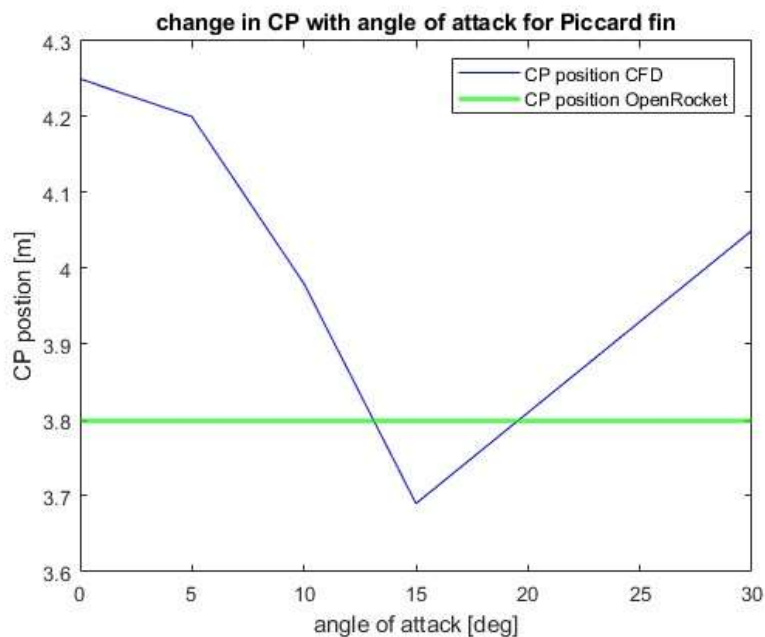

Figure 17 Change in CP location with a change in angle of attack for the Piccard fin
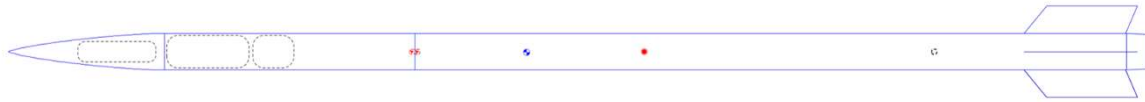
5.4 Swept back fins

CFD

The swept fins mesh had a cell count of 2 566 730 cells. Moreover, the mean orthogonal quality of the mesh lied within 0.74. Furthermore, 7% of the cells showed an orthogonality of less than 0.5. Nonetheless, the calculations converged after 53 iterations. All residuals show a converged status and lie bellow 10^-3. Lastly, as already seen in the previous simulations, the Y+ values lie well below 200. For the

swept back fins the Y+ values lied between 10 and 17 with some exceptions as can be seen in figure 31 in the appendix.

Aerodynamics

Stability: 3,2 cal
🌐 CG: 253 cm
🔴 CP: 310 cm

Figure 18 OpenRocket model of the Helvetia sounding rocket with Swept back fin configuration

As can be seen in figure 19 the initial location of the CP was 0.8 meters behind the CP estimated by OpenRocket. However, the CP shifts rearwards again as the a.o.a increases. Already at 10° a.o.a the CP is in front of the 3.1 meters that were estimated by OpenRocket. As can be seen in figure 31 in the appendix the lowest static margin is at 15° a.o.a with a value of 2.1 body callipers. By further increasing the angle of attack the CP moves rearwards to 3.4 meters at 30° a.o.a.
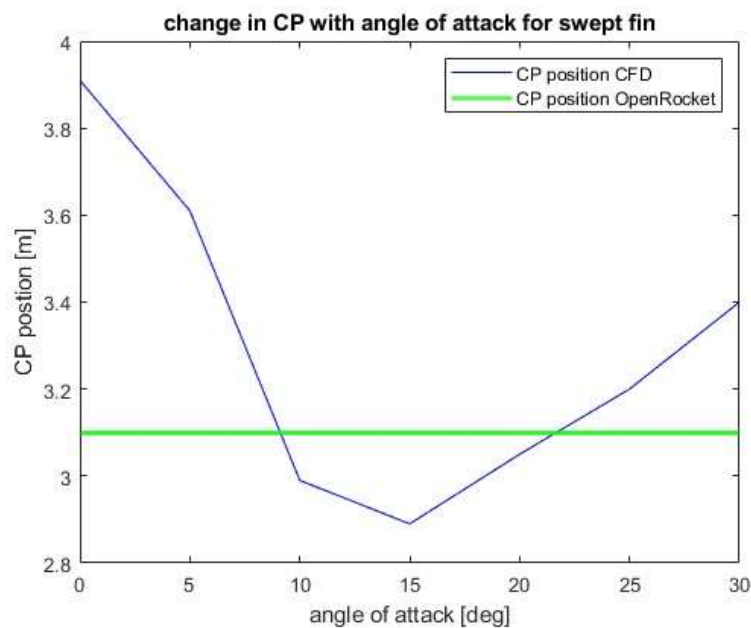

Figure 19 Change in CP with a change in angle of attack for the swept fin configuration

5.5 Overall comparison

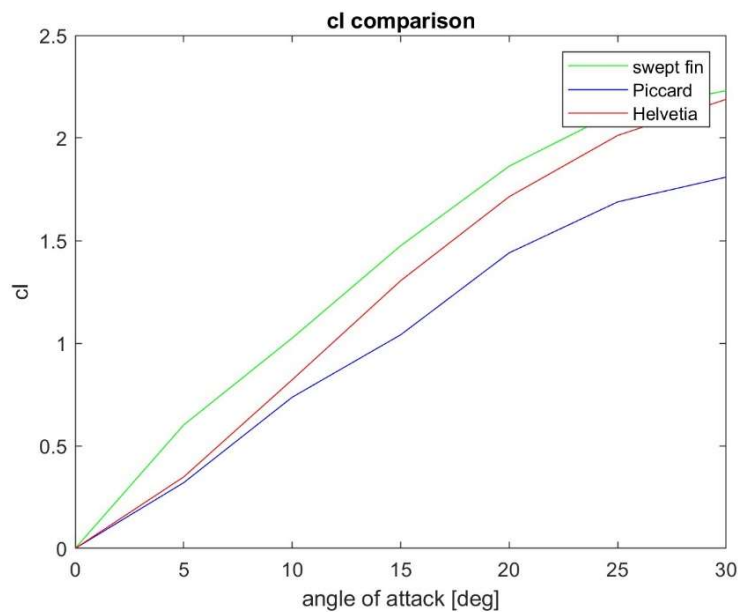Lastly, the lift and drag characteristics of the three fin shapes are compared.

Figure 20 coefficient of lift comparison of all fins

In figure 20 the Cl values for each fin is visualized. The swept fins have the highest overall Cl values whereas the Piccard fins have the lowest. A trend is visible that the Helvetia fins Close in on the swept ones as the angle of attack increases. The Piccard fins on the other hand show a nonlinear growth as early as 10° angle of attack, hinting at delamination.
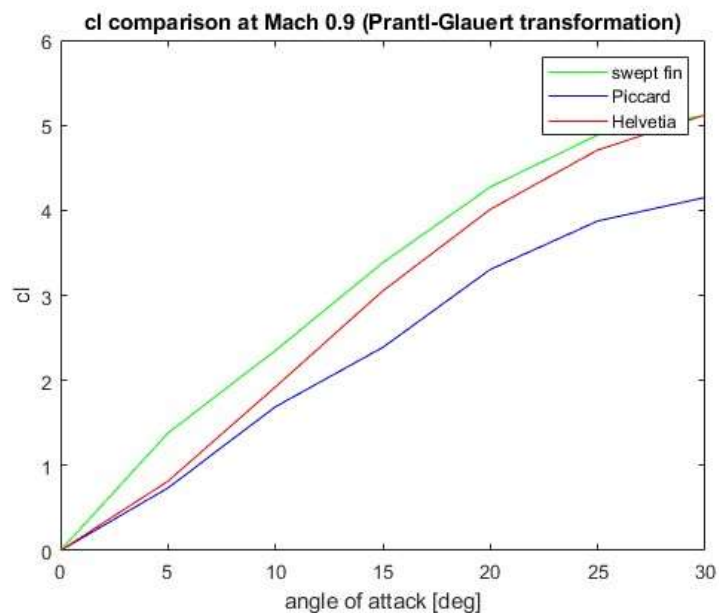

Figure 21 Prandtl-Glauert transformation (subsonic) comparison of Cl values of all fins

As can be seen in figure 21 all Cl values are higher in subsonic conditions compared to supersonic as in figure 20. The Prantl-Glauert factor is 0.44. Thus, the Cl values more than double from Mach 1.2 to Mach 0.9.

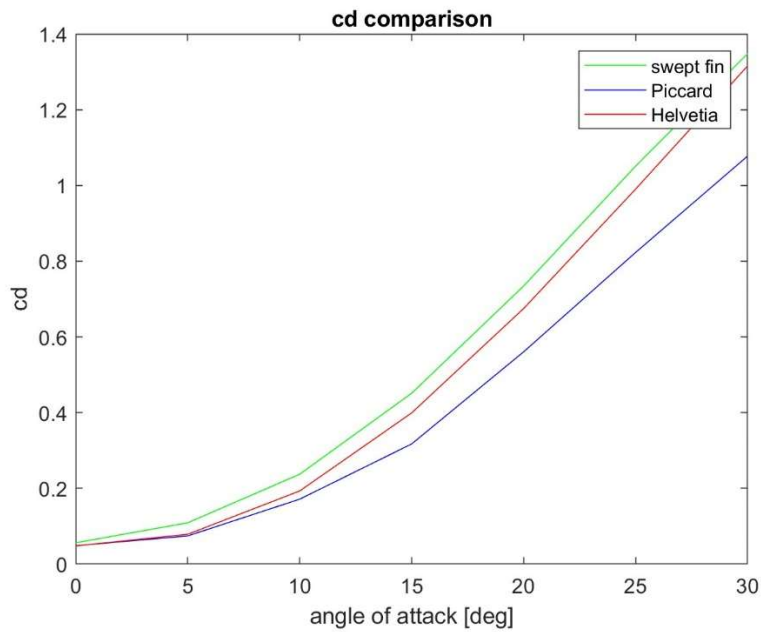*Figure 22 coefficient of drag comparison of all fins*

In figure 22 the Cd values for all three fin shapes are compared. The Piccard fins yield the least amount of drag. The drag difference between the Helvetia and the swept fin lies between 5 to 10%. On the other hand, the peak drag of the Piccard is almost 30% less than the drag of the other two fins.
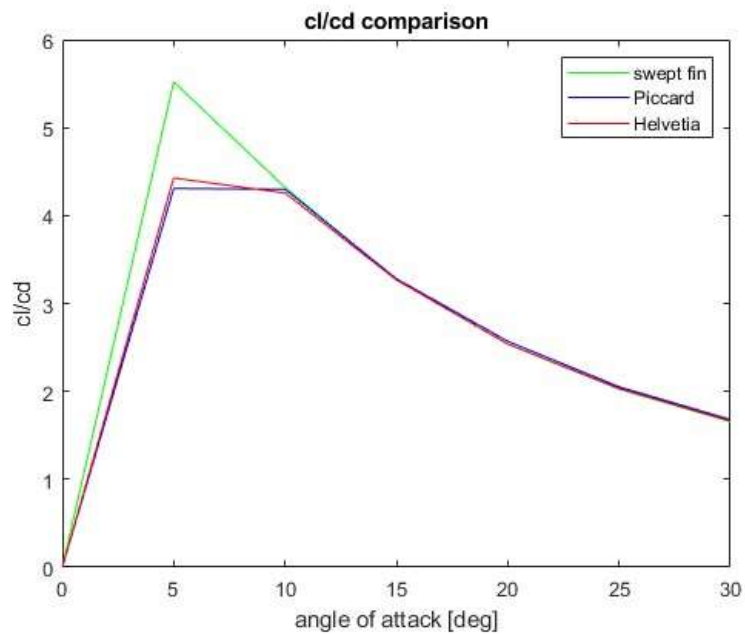

Figure 23 Cl over Cd comparison of all fins

Ultimately, the Cl over Cd values are compared as is visible in figure 23. The Piccard and Helvetia fins show an almost identical curve. Moreover, their highest lift over drag value reaches 4.2 and 4.3 for the Helvetia fin respectively. The swept fin on the other hand, shows a steeper gradient from 0° to 5° a.o.a than the other two fins. The maximum value of the swept fins lies at 5.6. Lastly, one can notice that for all fins the maximum lift to drag ratio is reached at an angle of attack of 5°.

6 Discussion

6.1 Nasa canard validation

Lift and drag

As can be seen in figure 10 the Cl values of the own CFD simulation and the reference CFD case from Youtube are nearly identical. However, both curves show slightly higher Cl values than the wind tunnel test. Given that the two CFD cases show the same deviation one can suspect that this is due to a natural discrepancy between the two research methods. On the other hand, it is possible that the turbulence intensity within the PFF would need to be adjusted to receive results that are closer to the wind tunnel test. Lastly, it may also be possible that minor measurement errors of the NASA wind tunnel test caused the deviation. Nonetheless, given that the calculations show only minor differences it can be assumed that the Cl values are realistic.

However, the Cd values from the own CFD simulation vary quite substantially from the reference CFD case. Most likely this is due to some issues with the mesh near the boundary layer. It would also explain why the Cl over Cd curve shows the deviation of almost 20%.

Y+

As can be seen in figure 28 in the appendix, the Y+ values were far below the aim of 200. A possible explanation for this is that the grid resolution near the boundary layer was insufficient. This hypothesis can be backed up as the maximum aspect ratio of the cells in that region reached a value of 150. However, it seems that this had no impact on the calculation of the lift coefficient. However, as can be seen in the drag calculations it is a possible explanation for the deviation from the reference case. For future studies it would make sense to change the meshing strategy in that area. In other words, the inner BOI would need to have a grow rate itself. Therefore, it is possible to create very small cells near the boundary layer yet have increasingly larger cells at the edge of the BOI to save computational power.

Static margin

In figure 25, in the appendix, one can immediately recognize that the location of the CP is quite differently evaluated by OpenRocket in comparison to the CFD simulation. The CP is evaluated to be further in front than is predicted by OpenRocket. Moreover, regarding figure 13 the missile becomes unstable at an a.o.a of 17°. This was unexpected. However, the pitching moment coefficients evaluated by NASA [22] is always negative. Which in turn means that the missile is always statically stable.

There are two explanations for this. Firstly, the mesh has major flaws and the deviation seen in the Cd evaluation had a similar impact on the center of pressure. However, except for the change in CP from 0° to 5° a.o.a the curve looks as expected. The CP moves forward until the fins starts stalling which is when the CP moves rearwards again. Therefore, there may be another possible explanation for the discrepancy. The NASA missile is guided, and the canard fins are all moving while the tail fins are fixed. For a Cl evaluation this has no impact. The Cl values were calculated given the lift force of the fins only. However, when it comes to the pitching moment, the entire rocket must be modelled correctly. However, in case of the CFD evaluation the canard fins remained fixed as well. Therefore, the CFD results show the point at which the missile would become unstable hadn't there been the canard fins that counteract the decreasing pitch moment. Lastly, this explanation can be backed up by the fact that according to Fan *et al.* [25], guided missiles are often designed by a concept known as controlled instability. According to this concept, the missile can be steered even when it is theoretically unstable.

In conclusion, the Cl values were accurate which hints at a robust mesh, However, the Cd values were off the reference value which in turn suggests an insufficient mesh near the boundary layer. Ultimately, the CP evaluation may be accurate for the given setup of the CFD simulation. Hence indicating some accuracy differences between OpenRocket and CFD. However, the CFD simulation did not incorporate the same configuration as the wind tunnel setup, since the canard fins were set as fixed. In order to receive the same results in terms of pitching moment as in the NASA test the canard fins would need to be adjusted for every change in angle of attack.

6.2 Fin comparison

CFD

In terms of mesh quality, it can be said that all mesh for the different fin shapes showed a similar robustness as the NASA canard mesh. Nonetheless, a common issue was once again the Y+ value. While it didn't reach the extent observed in the canard mesh, it still fell beneath the intended value. While a low Y+ would suggest an accurate model of the boundary layer it can be misleading. As previously stated, if the Y+ value is lower than expected, it mostly means that some of the cells have undesirable qualities. For example, high aspect ratio and low orthogonality. In addition, the Y+ is below 30 and yet larger than five which means it falls within the so-called buffer layer [10]. This in turn is not detrimental. However, it means that the velocity profile is not perfectly defined. It falls right between the viscosity dominated region which would correlate to Y+ values between 1 and 5 and the logarithmic wall function which is between 30 and 300. Therefore, the results need to be considered with some caution. On the other hand, the Y+ values have not fallen as low as in the NASA CFD case. This suggests that the cells at the edge of the boundary layer have a greater quality.

Ultimately, given the convergence of the results and the overall quality of the meshes, they were deemed usable without having to perform a mesh sensitivity analysis.

Nonetheless, for even more robust meshes, the cell count would most likely need to be within 20 million or more cells. However, this would restrict the quantity of simulations that could be run due to the limitation in computational power.

To sum up, a compromise was found between mesh quality and efficiency to run the many simulations that were conducted.

Aerodynamic forces

It was surprising to see that the swept fin showed the highest lift coefficients of the three fin designs. As the Helvetia fin has the largest surface it was the Clear favourite. However, it suggests that the parallelogram shape swept fin produces more lift per area than the trapezoid shaped Helvetia fin. Most likely this is because the trapezoid fin develops turbulence early on near the trailing edge whereas the swept fin delays the onset of this turbulence. Hence maintaining laminar flow. Unsurprisingly, the Piccard fin has the lowest Cl values. Given its extreme sweep angle and yet trapezoid shape it is designed for Mach numbers way above the envelope of the ARIS sounding rockets.

Regarding the Prandtl-Glauert transformation, seen figure 21, it can be said that the results must be considered with caution. It is evident that the Cl values increase from supersonic to the subsonic regime. Moreover, given that the same β was applied to all fins the Cl values increase proportionally. However, it is evident that under real conditions the Cl values would not change proportionally. All three fins have unique properties and would yield different Cl values in reaction to a shift from supersonic to subsonic. In addition, the Prandtl-Glauert transformation is most accurate in the transonic regime [16]. Meaning a shift in Mach number between 0.95 and 1.05. Hence the purpose of this transformation must be regarded as a demonstration and not as a scientific evaluation.

Considering the Cd comparison, it was unexpected to see that the swept fin yields the highest Cd value. A possible explanation for this is the before mentioned Y+ value which is within the buffer layer. In other words, the boundary layer was not dissolved perfectly. In addition, this can be explained by the orthogonal quality of the mesh which was the poorest for the swept fin mesh. Nonetheless, it is possible that the sweep angle would need to be increased further to sufficiently prevent the formation of shock waves. As expected, the Piccard fin has the lowest drag values overall. Proving that the fin was designed for higher speeds.

Lastly, the lift over drag curves yield a profound insight into the performance of the fins. The Piccard and Helvetia fins have a nearly identical curve, with a maximum lift over drag value of 4.2 for Piccard and 4.25 for Helvetia respectively. The swept back fin however, yields a much higher maximum value of 5.6. Again, this result must be considered with caution. Nonetheless, it shows that parallelogram shape of the fin is most efficient at a Mach number of 1.2.

In general, it must be said that while the Cl curves regarding angle of attack are highly important for the design of missiles it is less practical for sounding rockets. Especially in the supersonic regime. Guided missiles can change direction and reach high angles of attack even at supersonic speeds. However, the sounding rocket should for the

most part fly at a low angle of attack. Hence a more practical indicator in the design of the fins is the drag value as well as the center of pressure.

Nonetheless, by concluding the lift and drag study, some insight into the aerodynamic characteristic of the various fin shapes was gained.

Static margin

Firstly, a similar pattern regarding the shift in CP in reaction to a change a.o.a can be observed for all fin shapes. This supports the theory mentioned in chapter 2.3.

Secondly, according to Barrowman [2], the CP shifts from an average location of 25% chord length in subsonic to 50% in supersonic condition. For the Helvetia fin that would mean a shift of 14.4 cm, given a mean chord length of 57.4 cm. According to the Helvetia technical report [7], the CP lies at 4.03 meters from the tip of the rocket after leaving the launch rail with a velocity of 30 m/s. Thus, the CP should in theory lie at around 4.17 meters in supersonic flow. As can be seen in figure 29, with CFD, the CP at 0° a.o.a was evaluated to be at 4.12 meters. This can be treated as a reasonable result and demonstrates the differences between CFD and Barrowman's analytical approach. In addition, it validates the CFD setup. On the other hand, the OpenRocket result differs substantially from the CP that was evaluated with CFD. A possible reason for this discrepancy may be an error that occurred when setting up the OpenRocket model. Especially, since ARIS evaluated the CP with OpenRocket it is surprising that the result in this study varies from their result as well. Nonetheless, it is a possibility that that OpenRocket provides significantly inaccurate results within the supersonic regime.

Furthermore, given the results gathered from the Helvetia fin the CP position at 0° a.o.a for the Piccard fin can be judged as reasonable as well. Especially, since the discrepancy between OpenRocket and the CFD value show a similar difference of roughly 0.5 meters. By comparing the Piccard with the Helvetia fin, one can see that for the Piccard fin, the CP is further back. This is surprising since the surface area of the Helvetia fin is almost three times the area of the Piccard fin. A possible explanation is that the trapezoid shape of the Helvetia fin in correlation with the mild sweep angle creates more turbulence than the Piccard fin. This assumption can be supported by the much higher cd value of the Helvetia fin in comparison to the Piccard fin.

However, it is important to note that the behaviour of the center or pressure in correlation with a delaminated airflow can also cause the exact opposite to happen. Especially, when structured vortices form, the CP will tend to move rearwards [16].

Lastly, the CP location of the swept fin is the most forward of all three fins. Yet the static margin is the largest. However, when an a.o.a is implemented, the swept fin causes the largest forward shift. Most likely, this is due to the cl values being the highest for the swept fins. Considering the static margin, some caution must be advised.

Specifically, for this this study it was deemed as sufficient to only implement mass points to approximate a suitable static margin. The reason for this is that the CG position serves more as a reference to demonstrate the effect of angle of attack on the

static margin. However, the mass distribution was changed for all three fins to reach the desired static margin of 3.3 and 2, respectfully in OpenRocket. Hence the static margin is the highest initially for the swept fin. However, for the real rocket it is less than with the Helvetia fin.

Therefore, the most meaningful parameters are the initial CP locations as well as the total forwards shift of the CP.
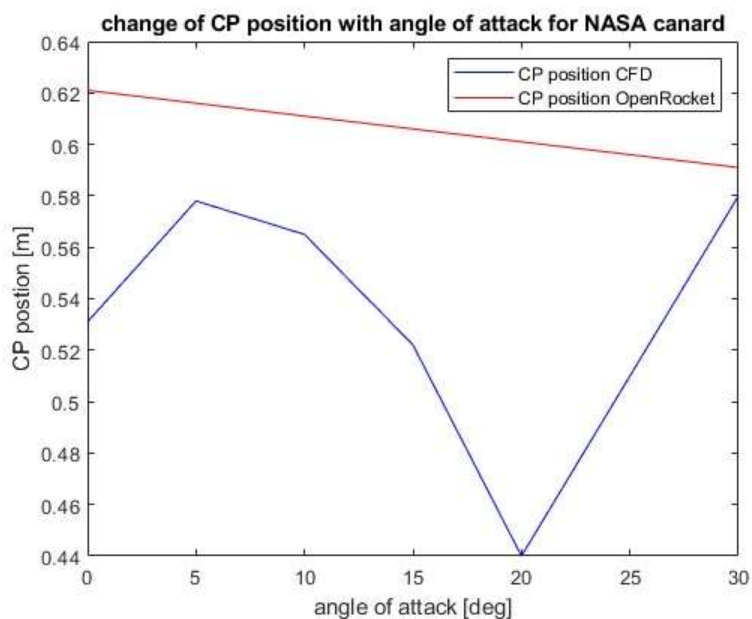
6.3 OpenRocket

Figure 24 Open rocket simulation of NASA canard missile: Cp position vs angle of attack

Within the scope of this thesis OpenRocket was only used to determine the CP position at an angle of attack of 0°. The reason for this is that the focus in this thesis lies on the CFD simulations. Moreover, OpenRocket shows a warning message when changing to a Mach number greater than one. Thus, suggesting that the results are inaccurate. Nonetheless, for comparative reasons one study was conducted as seen in figure 24. As expected, the results from OpenRocket are different than the ones gathered from the CFD simulation.

Firstly, the change of the CP position occurs linearly according to OpenRocket. This shows the limitations of the analytical model. Secondly, the critical angle of attack is reached at 70° in contrast to the suggested 20° obtained with CFD.

In summary, OpenRocket is an intuitive tool that can be used by hobbyists for model rockets that fly within the subsonic regime. Moreover, it can provide an accurate estimate of the static margin, even for larger rockets. However, for supersonic flow it is advisable to use CFD software instead.

7 Conclusion

Supersonic airflow is highly complex. However, CFD simulations make it possible to find reasonable solutions without making assumptions and simplifications to the model as it would need to be the case with analytical methods. Nonetheless, CFD simulations must be carefully set up as minor errors may cause large discrepancies with the results.

During this thesis the following lessons were learned.

Firstly, the boundary layer must be solved more carefully. It is most likely that this would result in a vastly larger cell count. Nonetheless, this is important to make the drag values more accurate.

Secondly, it is possible to accurately predict the CP for various a.o.a with CFD. However, to compare the static margin given the various fin shapes it is crucial to use the same mass distribution for all simulations.

Moreover, the OpenRocket software can be used at subsonic speeds. However, the software cannot accurately solve the complex fluid dynamics in supersonic conditions. Thus, relying on CFD is a better option.

Furthermore, the Prandtl-Glauert transformation is acceptable within the transonic regime. However, to find accurate lift values at speeds below Mach 0.9 an independent study must be conducted.

Lastly, it was demonstrated that lift and drag values can be found for rocket fins at supersonic speeds. This is important for fin design when the rocket or missile experiences high a.o.a in supersonic conditions. However, for ARIS sounding rockets only the drag value is crucial for the fin design. Cl and CP estimations are less meaningful in supersonic conditions. Cl and CP studies should be conducted at lows speeds matching the critical flight phases.

Regarding the various fin shapes the following was observed:

The swept fin proves to be less suitable for sounding rockets than the Helvetia fin. The reason for this is the large shift of center of pressure at an a.o.a. In addition, the high cd is an undesirable characteristic. Lastly, the CP location at 0° a.o.a would ideally be behind or at the same location as for the Helvetia fin. However, for guided missiles the fin may be the most suitable in comparison to the other fins. As the cl is the highest, it can make a missile highly maneuverable. Lastly, two key points need to be considered before reaching a final verdict. Firstly, the drag is most likely high due to the mesh. Secondly, the surface area is almost half of the Helvetia fin. By increasing the surface area and ultimately, making the mesh more robust a different result may be found.

Ultimately, the Piccard fin performs well at 0° a.o.a. However, it is less efficient than the Helvetia and the swept fin. Especially, when an a.o.a is implemented. Hence it can be said that the Piccard is more suitable for higher Mach numbers.

8 Outlook

For the mentioned reasons, in a future study the same fins may be examined at low speeds to find the aerodynamic characteristics during critical flight phases. Specifically, both during launch and during the rocket's gravity turn. During launch the rocket is most susceptible to wind gusts. Whereas, during the gravity turn the least amount of dynamic pressure is experienced. Thus, the rocket is at risk of becoming unstable as has happened to the Piccard rocket.

Moreover, in the future a combination of studies may be best for the optimization process of rocket fins. Namely a Cl and CP study at low speeds in combination with a supersonic study of the fin's drag. The low speed study should include a static margin analysis where the exact same mass distribution of the rocket is implemented for all fins.

In addition, a future study should incorporate the swept fin design but with a larger area as well as a slightly higher sweep angle. Within this thesis the performance of the swept fin was below expectations. However, by implementing the mentioned adjustments it could yield promising results.

Ultimately, a static stability analysis is only an initial step of the fin optimization process. A proceeding step would be to find the dynamic stability characteristics of the rocket fins. It is likely that while one fin performs well in static conditions it is unsuitable due to dynamic behavior. Therefore, a future study may incorporate the same fin shapes but implemented into a dynamic mesh CFD study.

9 Sources

[1] ARIS Space To Grow. "Main page." [Online]. Available: https://aris-space.ch/ (Accessed: June 9, 2023)

[2] J. S. Barrowman, "The Practical Calculation of the Aerodynamic Characteristics of Slender Finned Vehicles," M.S thesis, Dept. of Aerospace Engineering, Catholic University of America, Washington D.C, USA, 1967.

[3] M. Uliczka and I. Smykla, "Determining aircraft aerodynamic characteristics of regular and non-linear airframes and evaluating the efficiency of the applied methods," Journal of Physics: Conference Series, vol. 1736, no. 1. IOP Publishing, p. 012048, Jan. 01, 2021. doi: 10.1088/1742-6596/1736/1/012048.

[4] K. W. Saeed, S. A. Muttaleb, and J. Muhsin, "Comparison of Pressure Results between Wind Tunnel and CFD Simulation for University Baghdad Tower Building," International Journal of Modern Research in Engineering and Technology (IJMRET), vol. 5, no. 2, pp. 11, Mar. 2020. Available: www.ijmret.org, ISSN: 2456-5628.

[5] S. A. Mohammadein, R. A. Gad El-Rab, and M. S. Ali, "The Simplest Analytical Solution of Navier-Stokes Equations," Mathematics Department, Faculty of Science, Tanta University, Tanta, Egypt and Al-Ghad International Medical Sciences College, Najran, Saudi Arabia, Received: 21 Dec. 2020, Revised: 2 Jan. 2021, Accepted: 19 Jan. 2021, Published online: 1 May 2021.

[6] OpenRocket. (n.d.). "Main Page." OpenRocket Wiki. [Online] Available: http://wiki.openrocket.info/Main_Page (Accessed: June 9, 2023)

[7] Akademische Raumfahrt Initiative Schweiz. (2022). "Project HELVETIA: How to Fail and Still Succeed." Unpublished report, Akademische Raumfahrt Initiative Schweiz, Wangenstrasse 72 DFA, Halle 3, 8600 Dübendorf, Switzerland.

[8] Akademische Raumfahrt Initiative Schweiz. (2021) "Project PICCARD: Team 27 Project Technical Report for the 2021 Spaceport America Cup," Unpublished.

[9] S. M. Salim and S. C. Cheah, "Wall y+ Strategy for Dealing with Wall-bounded Turbulent Flows," presented at International MultiConference of Engineers and Computer Scientists, IMECS 2009

[10] H. Schlichting and K. Gersten, "Boundary-Layer Theory". Springer Berlin Heidelberg, 2017. doi: 10.1007/978-3-662-52919-5.

[11] H. K. Versteeg and Weeratunge Malalasekera, "An introduction to computational fluid dynamics: the finite volume method". Harlow: Pearson Education, 2007.

[12] Ansys Fluent 12.0 Theroy Guide. (n.d.). "Main Page." Ansys Wiki. [Online] Available: https://www.afs.enea.it/project/neptunius/docs/fluent/html/th/main_pre.htm (Accessed: June 9, 2023)

[13] NASA Glenn Research Center, "Isentropic Flow Relations," Grc.nasa.gov. [Online]. Available: https://www.grc.nasa.gov/www/BGH/isentrop.html. (Accessed: June 9, 2023)

[14] A. Seeni, P. Rajendran, and H. Mamat, "A CFD Mesh Independent Solution Technique for Low Reynolds Number Propeller," CFD letters, vol. 11, no. 10, pp. 15-30, 2019.

[15] NASA Glenn Research Center, "Beginner's Guide to Aeronautics: Lift-to-Drag Ratio," Grc.nasa.gov. [Online]. Available: https://www1.grc.nasa.gov/beginners-guide-to-aeronautics/lift-to-drag-ratio/. (Accessed: June 9, 2023)

[16] J. Anderson, "Fundamentals of Aerodynamics". McGraw-Hill education, New York, 2017. ISBN 978-1-259-12991-9

[17] A. H. Shapiro, "The Dynamics and thermodynamics of compressible fluid flow". Vol. 1, Massachusetts Institute of Technology, New York, 1953.

[18] Aero Toolbox "Intro to Sweep Angle," Aerotoolbox, [Online] Available: https://aerotoolbox.com/intro-sweep-angle/. (Accessed: June 9, 2023)

[19] O. Wright "Static Stability and Control". June 7, 1903 [Online] Available: https://home.engineering.iastate.edu/~shermanp/AERE355/lectures/Nelson%20Chapter%202.pdf (Accessed: June 9, 2023)

[20] S. Niskanen "OpenRocket technical documentation," For OpenRocket version 13.05 [Online] Available: https://openrocket.sourceforge.net/techdoc.pdf (Accessed: June 9, 2023)

[21] S. Niskanen The "Development of an Open Source model rocket simulation software" M.S thesis, Faculty of Information and Natural Sciences, Helsinki University of Technology, Helsinki, 2009.

[22] A. B. Blair Jr. "Wind-Tunnel Investigation at Supersonic Speeds of a Canard-Controlled Missile With Fixed and Free-Rolling Tail Fins", Nasa Technical Paper 1316, September 1978. [Online] Available: https://ntrs.nasa.gov/api/citations/19780024124/downloads/19780024124.pdf (Accessed: June 9, 2023)

[23] Ansys Space Claim (n.d.). "Main Page." Ansys SpaceClaim 3D Modeling Software. [Online] Available: https://www.ansys.com/products/3d-design/ansys-spaceclaim (Accessed: June 9, 2023)

[24] SimScale "Mesh Sensitivity in CFD," SimScale Knowledge Base. [Online]. Available: https://www.simscale.com/knowledge-base/mesh-sensitivity-cfd/. (Accessed: June 9, 2023)

[25] J. Fan, D. Lin, Z. Su, Q. Li, " Control of static unstable airframes" Journal of Systems Engineering and Electronics, vol. 21, no. 6, pp. 1063-1071, Dec 2010. [Online] Available: https://ieeexplore.ieee.org/stamp/stamp.jsp?arnumber=6077558 (Accessed: June 9, 2023)

10 Appendix

	Value	Absolute Criteria	Convergence Status
continuity	0.0009705789	0.001	Converged
x-velocity	7.363377e-08	0.001	Converged
y-velocity	6.61761e-08	0.001	Converged
z-velocity	7.878555e-08	0.001	Converged
energy	3.780541e-07	1e-06	Converged
k	0.0002061545	0.001	Converged
omega	0.000190089	0.001	Converged

Figure 25 convergence of the residuals of NASA canard CFD
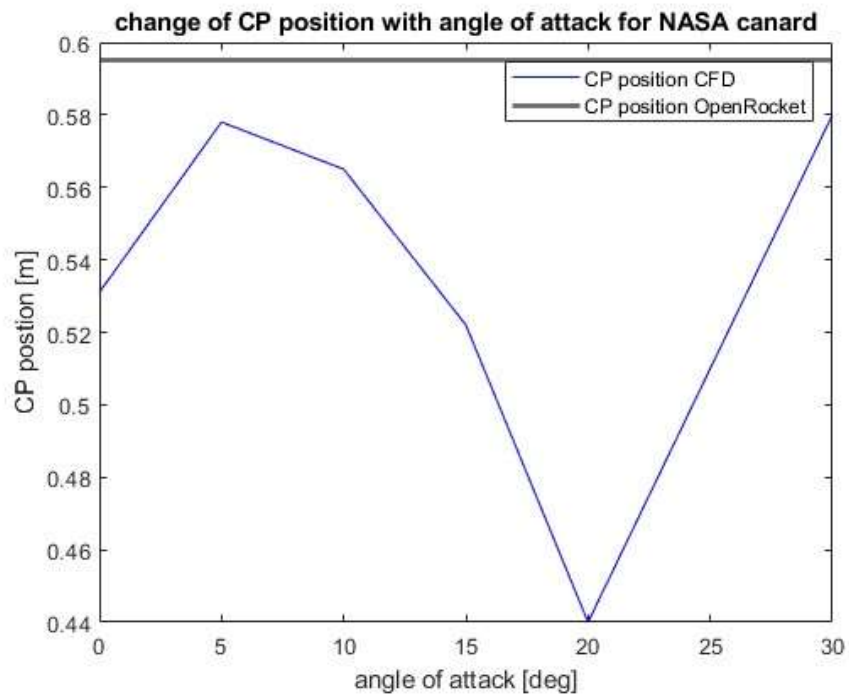
Figure 26 Change in CP position in relation with a change in angle of attack of the NASA canard missile
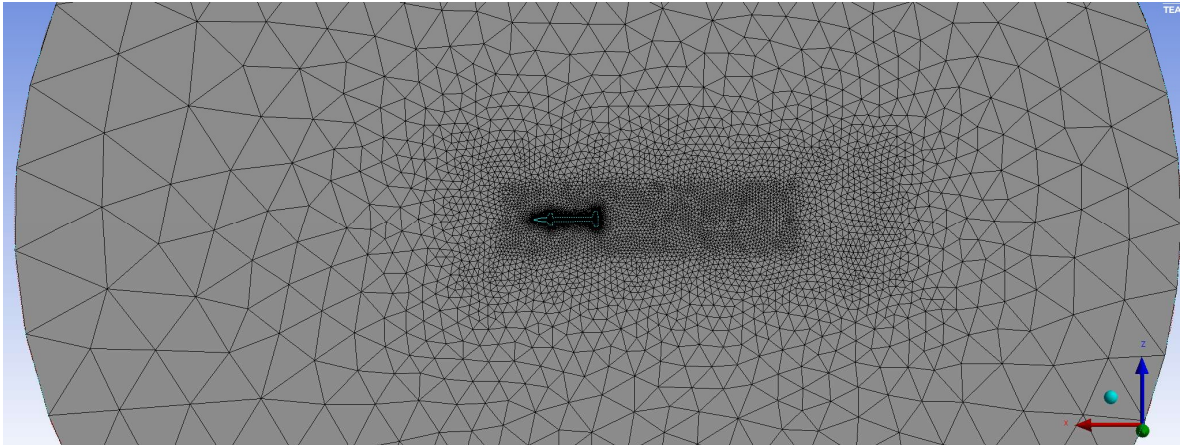
Figure 27 Nasa canard mesh
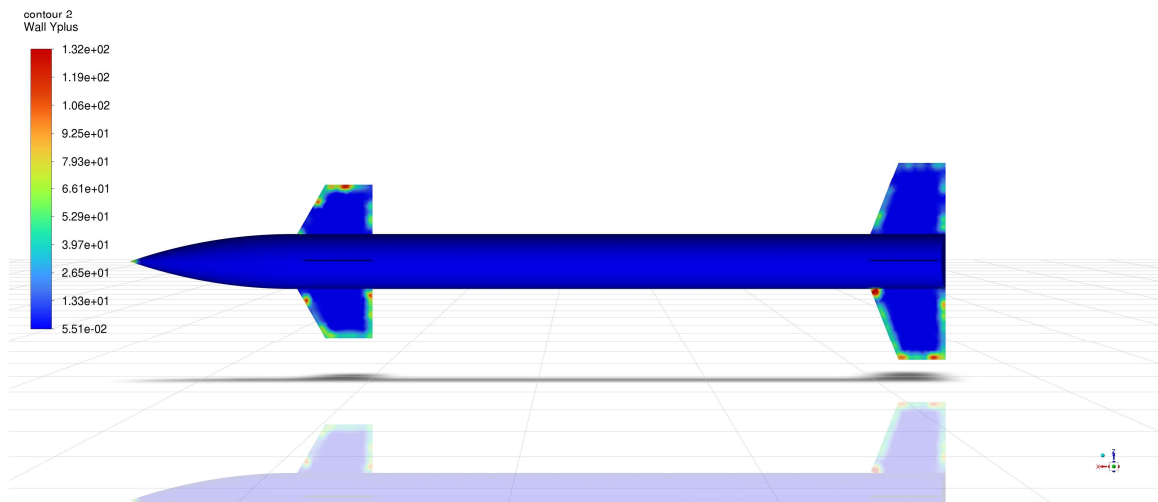
Figure 28 Y+ values of Nasa canard CFD
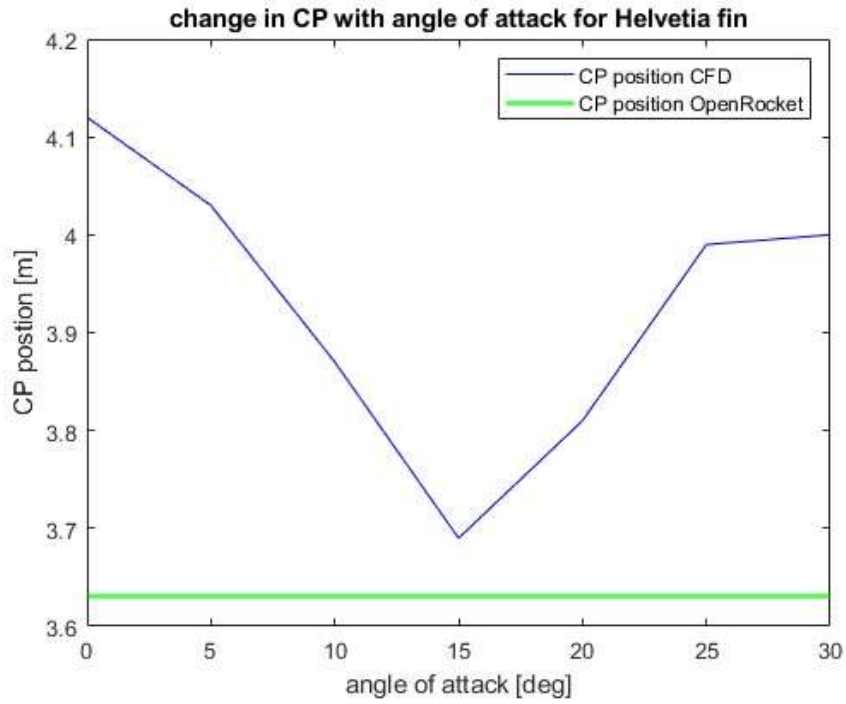
Figure 29 Change in CP location of Helvetia fin with a change in angle of attack
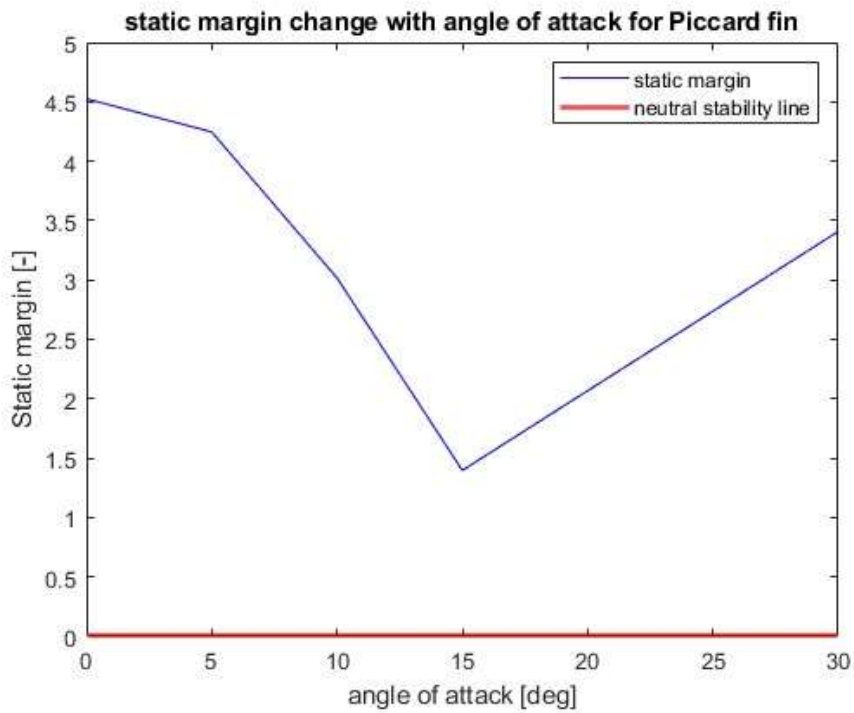

Figure 30 static margin change with angle of attack of Piccard fin
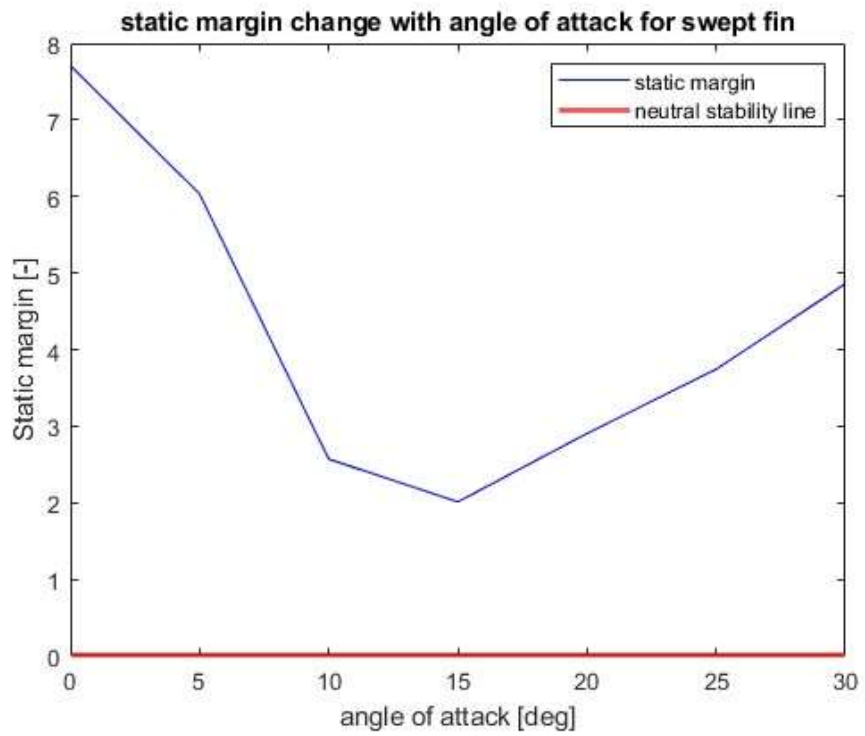
Figure 31 Y+ values of swept back fin

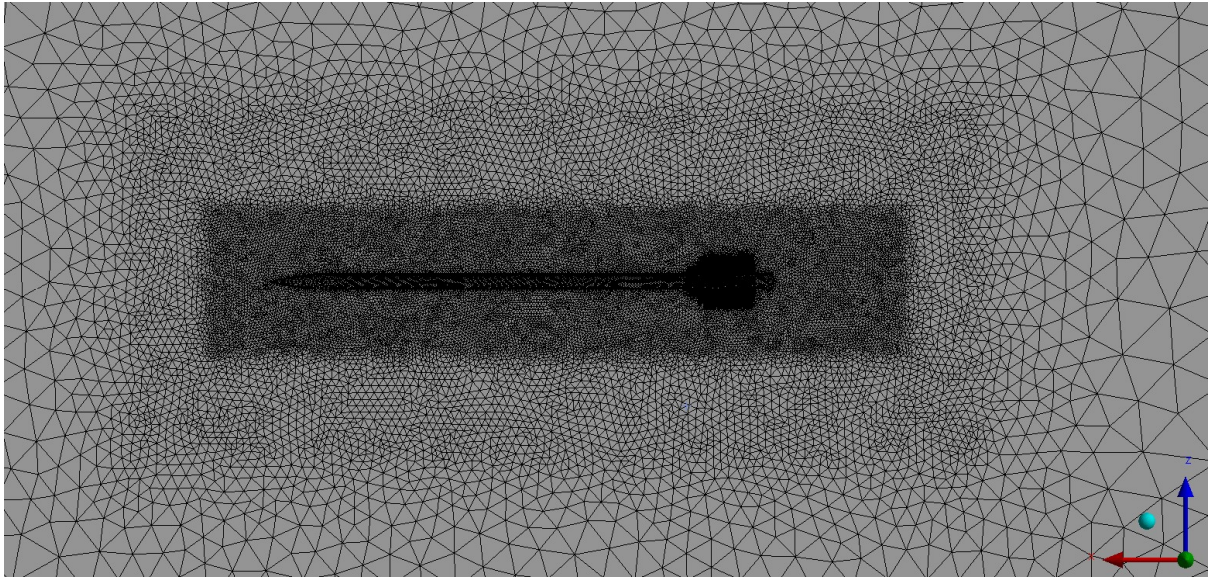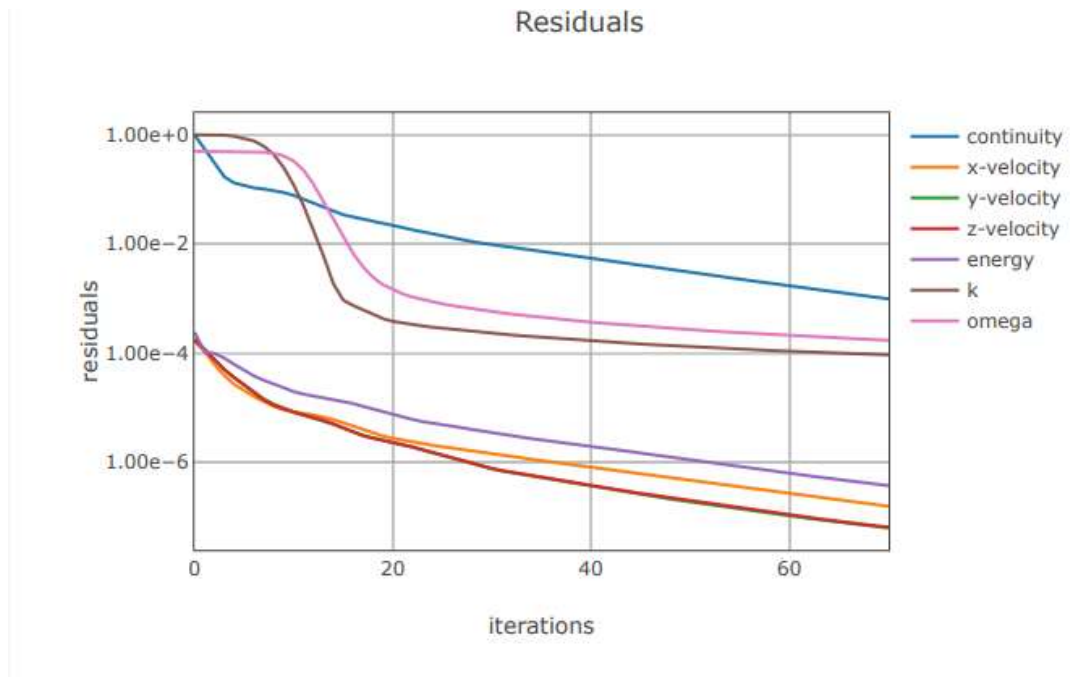*Figure 32 static margin shift with angle of attack for swept fin*

Figure 33 Helvetia mesh

Figure 34 residuals of Helvetia CFD simulation